

# Secure Intelligent Reflecting Surface Aided Integrated Sensing and Communication

Meng Hua, Qingqing Wu, *Senior Member, IEEE*, Wen Chen, *Senior Member, IEEE*, Octavia A. Dobre, *Fellow, IEEE*, and A. Lee Swindlehurst, *Fellow, IEEE*

**Abstract**—In this paper, an intelligent reflecting surface (IRS) is leveraged to enhance the physical layer security of an integrated sensing and communication (ISAC) system in which the IRS is deployed to not only assist the downlink communication for multiple users, but also create a virtual line-of-sight (LoS) link for target sensing. In particular, we consider a challenging scenario where the target may be a suspicious eavesdropper that potentially intercepts the communication-user information transmitted by the base station (BS). To ensure the sensing quality while preventing the eavesdropping, dedicated sensing signals are transmitted by the BS. We investigate the joint design of the phase shifts at the IRS and the communication as well as radar beamformers at the BS to maximize the sensing beampattern gain towards the target, subject to the maximum information leakage to the eavesdropping target and the minimum signal-to-interference-plus-noise ratio (SINR) required by users. Based on the availability of perfect channel state information (CSI) of all involved user links and the accurate target location at the BS, two scenarios are considered and two different optimization algorithms are proposed. For the ideal scenario where the CSI of the user links and the target location are perfectly known at the BS, a penalty-based algorithm is proposed to obtain a high-quality solution. In particular, the beamformers are obtained with a semi-closed-form solution using Lagrange duality and the IRS phase shifts are solved for in closed form by applying the majorization-minimization (MM) method. On the other hand, for the more practical scenario where the CSI is imperfect and the target location is uncertain, a robust algorithm based on the  $S$ -procedure and sign-definiteness approaches is proposed. Simulation results demonstrate the effectiveness of the proposed scheme in achieving a trade-off between the communication quality and the sensing quality, and also show the tremendous potential of IRS for use in sensing and improving the security of ISAC systems.

**Index Terms**—Intelligent reflecting surface, integrated sensing and communication, robust design, physical layer security, transmit beamforming.

## I. INTRODUCTION

Driven by emerging applications for high-accuracy sensing services such as autonomous driving, robot navigation, and intelligent traffic monitoring, etc., a new paradigm is required to shift from communication-based network designs to networks with sensing-communication integration [1]. The research on the integration of sensing and communication networks has recently attracted significant attention along the following two directions: radar-communication coexistence [2] and integrated sensing and communication (ISAC) [3]. In the former, the radar transceiver and the communication transmitter are geographically separated, which usually results in strong co-channel interference and

requires prohibitive feedback overhead to exchange information for coordination between two systems. For the latter, the radar and communication functionalities share a common hardware platform, which leads to both integration and coordination gains.

Recently, we are witnessing a booming interest from both academia and industry on ISAC systems due to their reduced hardware cost, lower power consumption, and more efficient radio spectrum usage [4]. Based on design priorities and underlying requirements, ISAC systems can be classified into three categories: communication-centric (C&C) designs [5], radar-centric (R&C) designs [6], and joint waveform designs [7]–[9]. For C&C design, the sensing functionality is integrated into the existing communication platform, where the communication performance has the highest priority. The objective of this type of design is to exploit the communication waveform to implement the sensing functionality while satisfying the quality-of-service (QoS) of the communication users. In contrast to the C&C design, sensing has the highest priority in R&C designs. The objective of this approach is to modulate the information into the sensing waveform to realize the communication functionality without significantly degrading the sensing performance. The performance of the two types of designs above is fundamentally limited by the hardware platforms and signal processing algorithms and fails to achieve a scalable tradeoff between sensing and communication. The last category, i.e., joint waveform design, creates new waveforms instead of relying on existing communication or radar waveforms, and provides additional degrees of freedom (DoFs) to support high data rates and to improve sensing quality. As an example of the joint design approach, the authors in [7] revealed that communication-only waveform design is inferior to the joint design of communication and radar waveforms in terms of beampattern synthesis, especially when the number of communication users is less than the number of targets. However, the ISAC system performance is significantly deteriorated by unfavorable propagation environments with signal blockages, especially for target sensing. In general, only the reflected echo signals that pass through line-of-sight (LoS) links are treated as useful information for sensing while non-LoS (NLoS) links are treated as harmful interference or clutter. Unmanned aerial vehicles (UAVs) have been leveraged to assist ISAC systems since the UAV can establish strong LoS links between the UAV and users/targets by adjusting its trajectory or deployment [10]–[13]. However, the UAV-enabled ISAC is not suitable for providing long-term coverage due to the inherently limited battery capacity available on a UAV. This raises a new open question: How to provide long-term and ubiquitous sensing coverage in harsh environments where the channel links are blocked in the ISAC system?

Recently, intelligent reflecting surface (IRS) technology has attracted significant attention and is regarded as a promising technology towards for beyond-fifth-generation (B5G) and sixth-generation (6G) systems, due to its capability of manipulating

M. Hua and Q. Wu are with the State Key Laboratory of Internet of Things for Smart City, University of Macau, Macao 999078, China (email: menghua@um.edu.mo; qingqingwu@um.edu.mo).

W. Chen is with the Department of Electronic Engineering, Shanghai Institute of Advanced Communications and Data Sciences, Shanghai Jiao Tong University, Minhang 200240, China (e-mail: wenchen@sjtu.edu.cn).

O. A. Dobre is with the Faculty of Engineering and Applied Science, Memorial University, St. John's, NL A1B 3X5, Canada (email: odobre@mun.ca).

A. L. Swindlehurst is with the Center for Pervasive Communications and Computing, University of California at Irvine, Irvine, CA 92697 USA (e-mail: swindle@uci.edu).

the wireless propagation environment with low power consumption and hardware cost [14], [15]. Specifically, an IRS is a two-dimensional planar array comprising a large number of sub-wavelength metallic units, each of which is able to independently control the phases and/or amplitudes of impinging signals. Due to the small size of each reflecting unit, a reasonably-sized IRS can be constructed with a large number of reflecting elements and can provide significant beamforming gains to compensate for signal attenuation over long distances [16]. Motivated by this, IRS technology has been extensively investigated in the literature for various applications such as mobile edge computing (MEC) [17]–[19], wireless power transfer [20]–[23], and multi-cell cooperation [24]–[26]. The use of IRS is very appealing for ISAC since it is able to create virtual LoS links for both communication and sensing. Some representative works, see e.g., [27]–[29], have studied the use of IRS for sensing and verified their potential for enhancing target sensing. A handful of related works have been conducted on IRS-aided ISAC in the literature, see [30]–[34], via jointly optimizing IRS phase shifts and transmit beamformers to increase the sensing quality while satisfying communication QoS of the users. However, the above works assumed that the targets are not attempting to intercept the transmitted signals. In ISAC systems, the transmitted signals may not only contain sensing signals but also communication signals, which could be readily intercepted by malicious targets. The problem of maintaining the communication QoS and the target sensing performance while also ensuring limited information leakage to the targets has received very little attention. Although works [35] and [36] studied secure transmission designs for ISAC system, the role of IRS for sensing and communication was not unveiled and their proposed transceiver designs are also no longer applicable in the presence of an IRS.

Motivated by the above issues, in this paper we study a secure IRS-aided ISAC system where the IRS is leveraged to not only assist the downlink communication from the base station (BS) to multiple legitimate users, but to also create a virtual LoS link for target sensing. In addition, we consider a challenging scenario where the target may be an eavesdropper that desires to intercept information transmitted by the BS. The main contributions of this paper are summarized as follows:

- We study an IRS-aided ISAC system for enhancing the physical layer security and realizing both communication and sensing. To ensure the sensing quality while preventing eavesdropping, dedicated sensing signals are transmitted at the BS. Our objective is to maximize the sensing beampattern gain by jointly optimizing the communication beamformers, radar beamformers, and IRS phase shifts, subject to the maximum tolerable information leakage to the eavesdropping target and the minimum signal-to-interference-plus-noise ratio (SINR) required by the users. Based on whether or not perfect channel state information (CSI) and target location information are known by BS, two different optimization problems are formulated. Subsequently, two different algorithms are proposed, i.e., a penalty-based algorithm and a robust algorithm.
- For the ideal scenario where the CSI of the user links and the target location are known at the BS, the resulting optimization problem is non-convex due to the presence of coupled optimization variables in both the objective function and constraints. In addition, the unit-modulus constraint imposed on each IRS phase shift renders the formulated problem more difficult to solve. To address

this difficulty, a penalty-based algorithm is proposed in which the beamformers are obtained with a semi-closed-form solution using Lagrange duality and the IRS phase shifts are obtained with a closed-form solution by applying majorization-minimization (MM), both of which significantly reduce the computational complexity of the penalty-based algorithm.

- For the more practical scenario where perfect CSI of communication channels and the target location are not available at the BS, we design a robust transmission strategy. The resulting optimization problem involving an infinite number of constraints is more challenging to solve than the former one, and the previous penalty-based algorithm is no longer applicable. To solve this optimization problem, the  $\mathcal{S}$ -procedure and sign-definiteness approaches are applied to transform the infinite number of inequalities into a finite number of linear matrix inequalities (LMIs). Then, an efficient alternating optimization (AO) algorithm is proposed that toggles between optimizing the transmit beamformers and IRS phase shifts.
- Our simulation results verify the effectiveness of the proposed scheme in achieving a trade-off between the communication quality and the target sensing quality and validate the tremendous potential of IRS to achieve significant beampattern gains and guarantee ISAC system security. Our results also show that dedicated sensing signals are required to further improve the system performance.

The rest of the paper is organized as follows. Section II introduces the system model and problem formulations for the considered IRS-aided secure ISAC system. In Section III, a penalty-based algorithm is proposed to solve the perfect CSI and the known-target location case. In Section IV, a robust design algorithm is proposed to solve the case with imperfect CSI and uncertain target location. Numerical results are provided in Section V and the paper is concluded in Section VI.

*Notations:* Boldface upper-case and lower-case letters denote matrices and vectors, respectively.  $\mathbb{C}^{d_1 \times d_2}$  stands for the set of complex  $d_1 \times d_2$  matrices. For a complex-valued vector  $\mathbf{x}$ ,  $\|\mathbf{x}\|$  represents the Euclidean norm of  $\mathbf{x}$ ,  $\arg(\mathbf{x})$  denotes a vector containing the phase of the elements of  $\mathbf{x}$ , and  $\text{diag}(\mathbf{x})$  denotes a diagonal matrix whose diagonal elements are given by the elements of  $\mathbf{x}$ .  $(\cdot)^T$ ,  $(\cdot)^*$ , and  $(\cdot)^H$  stand for the transpose operator, conjugate operator, and conjugate transpose operator, respectively.  $\|\mathbf{X}\|_F$  and  $\text{rank}(\mathbf{X})$  represent the Frobenius norm and rank of  $\mathbf{X}$ , respectively, and  $\mathbf{X} \succeq \mathbf{0}$  indicates that matrix  $\mathbf{X}$  is positive semi-definite. A circularly symmetric complex Gaussian random variable  $x$  with mean  $\mu$  and variance  $\sigma^2$  is denoted by  $x \sim \mathcal{CN}(\mu, \sigma^2)$ .  $\otimes$  denotes the Kronecker product operator and  $\mathcal{O}(\cdot)$  indicates the big-O computational complexity.

## II. SYSTEM MODEL AND PROBLEM FORMULATION

### A. System Model

We consider a secure IRS-aided ISAC system that comprises a dual-function BS, an IRS, one target of interest,<sup>1</sup> and  $K$  single-antenna users, as shown in Fig. 1. The BS is equipped with a uniform linear array with  $N$  transmit antennas, and the IRS is a uniform planar array with  $M$  reflecting elements. For

<sup>1</sup>Although we consider a single target in this work, the algorithms proposed for the single-target case are applicable to the multi-target case with only slight modifications.

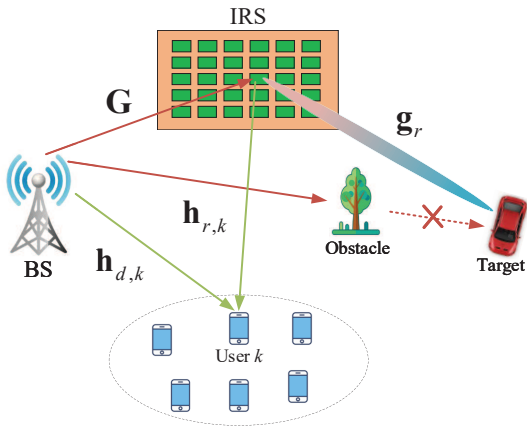


Fig. 1. An IRS-aided secure ISAC system.

convenience, we denote the sets of users, BS transmit antennas, and IRS reflecting elements as  $\mathcal{K}$ ,  $\mathcal{N}$ , and  $\mathcal{M}$ , respectively.

We assume that both information signals and radar signals are simultaneously transmitted for communication and sensing. The transmitted signals at the BS can be expressed as

$$\mathbf{s} = \sum_{k=1}^K \mathbf{w}_{c,k} x_{c,k} + \sum_{n=1}^N \mathbf{w}_{r,n} x_{r,n}, \quad (1)$$

where  $x_{c,k}$  denotes the information signal for user  $k$  assumed to satisfy  $x_{c,k} \sim \mathcal{CN}(0, 1)$  and  $\mathbf{w}_{c,k} \in \mathbb{C}^{N \times 1}$  represents its corresponding communication beamformer. Similarly,  $x_{r,n}$  denotes the  $n$ th radar signal satisfying  $\mathbb{E}\{x_{r,n}\} = 0$  and  $\mathbb{E}\{|x_{r,n}|^2\} = 1$ , and  $\mathbf{w}_{r,n} \in \mathbb{C}^{N \times 1}$  represents the corresponding radar beamformer. We assume that communication and radar signals are statistically independent and uncorrelated, i.e.,  $\mathbb{E}\{x_{r,n} x_{c,k}^H\} = 0, \forall k, n$ .

1) *Communication Model*: We consider quasi-static block-fading channels and focus on a given fading block during which all the channels involved are assumed to remain unchanged. Let  $\mathbf{G} \in \mathbb{C}^{M \times N}$  denote the complex equivalent baseband channel from the BS to the IRS,  $\mathbf{h}_{r,k}^H \in \mathbb{C}^{1 \times M}$  denote that from the IRS to user  $k$ , and  $\mathbf{h}_{d,k}^H \in \mathbb{C}^{1 \times N}$  denote that from the BS to user  $k$ ,  $k \in \mathcal{K}$ . We assume that the CSI of all involved channels, i.e.,  $\mathbf{G}$ ,  $\text{diag}(\mathbf{h}_{r,k}^H) \mathbf{G}$ , and  $\mathbf{h}_{d,k}^H$ , is available at the BS by applying channel estimation methods, e.g., [37]. The signal received at user  $k$  is given by

$$y_k = (\mathbf{h}_{r,k}^H \mathbf{\Theta} \mathbf{G} + \mathbf{h}_{d,k}^H) \mathbf{s} + n_k, k \in \mathcal{K}, \quad (2)$$

where  $\mathbf{\Theta} = \text{diag}(v_1, \dots, v_M)$  represents the IRS reflection phase shift matrix and  $n_k \sim \mathcal{CN}(0, \sigma_k^2)$  denotes the noise received at user  $k$ . Accordingly, the received SINR at user  $k$  is given by

$$\gamma_k = \frac{|\mathbf{h}_k^H \mathbf{w}_{c,k}|^2}{\sum_{i \neq k} |\mathbf{h}_k^H \mathbf{w}_{c,i}|^2 + \sum_{n=1}^N |\mathbf{h}_k^H \mathbf{w}_{r,n}|^2 + \sigma_k^2}, k \in \mathcal{K}, \quad (3)$$

where  $\mathbf{h}_k^H = \mathbf{h}_{r,k}^H \mathbf{\Theta} \mathbf{G} + \mathbf{h}_{d,k}^H$ .

2) *Radar Sensing and Interception Model*: We consider the scenario where the direct link between the BS and the potential target is not available due to the blockages. To tackle this issue, the IRS is leveraged to create a virtual LoS link between the IRS and the target, thereby establishing an effective BS-IRS-target link for sensing. Let  $\theta$  and  $\varphi$  denote the azimuth and elevation angle-of-departure (AoD) from the IRS to the target,

respectively. Accordingly, the steering vector from the IRS to the target at direction  $(\theta, \varphi)$  can be expressed as

$$\mathbf{g}_r^H = \alpha_r \left[ 1, e^{-j \frac{2\pi d}{\lambda} \sin \theta \cos \varphi}, \dots, e^{-j \frac{2\pi (M_x - 1)d}{\lambda} \sin \theta \cos \varphi} \right] \otimes \left[ 1, e^{-j \frac{2\pi d}{\lambda} \sin \theta \sin \varphi}, \dots, e^{-j \frac{2\pi (M_z - 1)d}{\lambda} \sin \theta \sin \varphi} \right], \quad (4)$$

where  $M_x$  and  $M_z$  denote the numbers of reflecting elements along  $x$ -axis and  $z$ -axis, respectively,  $\alpha_r$  represents the large-scale fading coefficient,  $\lambda$  denotes the wavelength, and  $d$  denotes the spacing between two adjacent reflecting elements. The received signal at the target is given by

$$y_t = \mathbf{g}_r^H \mathbf{\Theta} \mathbf{G} \left( \sum_{k=1}^K \mathbf{w}_{c,k} x_{c,k} + \sum_{n=1}^N \mathbf{w}_{r,n} x_{r,n} \right) + n_t, \quad (5)$$

where  $n_t \sim \mathcal{CN}(0, \sigma_t^2)$  represents the noise received at the target. As a result, the beampattern gain towards the target is given by

$$\mathcal{P} = \mathbb{E} \left\{ \left| \mathbf{g}^H \left( \sum_{k=1}^K \mathbf{w}_{c,k} x_{c,k} + \sum_{n=1}^N \mathbf{w}_{r,n} x_{r,n} \right) \right|^2 \right\} = \mathbf{g}^H \left( \sum_{k=1}^K \mathbf{w}_{c,k} \mathbf{w}_{c,k}^H + \sum_{n=1}^N \mathbf{w}_{r,n} \mathbf{w}_{r,n}^H \right) \mathbf{g}, \quad (6)$$

where  $\mathbf{g}^H = \mathbf{g}_r^H \mathbf{\Theta} \mathbf{G}$ .

Since the target is a potential eavesdropper, it tries to decode information from its received signals. The SINR received at the target for intercepting user  $k$ 's information is given by

$$\gamma_{e,k} = \frac{|\mathbf{g}^H \mathbf{w}_{c,k}|^2}{\sum_{i \neq k} |\mathbf{g}^H \mathbf{w}_{c,i}|^2 + \sum_{n=1}^N |\mathbf{g}^H \mathbf{w}_{r,n}|^2 + \sigma_t^2}, k \in \mathcal{K}. \quad (7)$$

## B. Problem Formulation

The objective of this paper is to maximize the beampattern gain at the target by jointly optimizing the transmit beamformers and IRS phase shifts, subject to the minimum SINR required by users and the maximum tolerable information leakage to the target. Depending on whether perfect CSI of the communication channels and the target location are available at the BS, we consider two scenarios elaborated as below.

1) *Perfect CSI and Known Target Location Scenario*: In this scenario, perfect CSI of the communication channels and the target location are known at the BS. Accordingly, the problem is formulated as

$$\max_{\{\mathbf{w}_{c,k}, \mathbf{w}_{r,n}, v_m\}} \mathbf{g}^H \left( \sum_{k=1}^K \mathbf{w}_{c,k} \mathbf{w}_{c,k}^H + \sum_{n=1}^N \mathbf{w}_{r,n} \mathbf{w}_{r,n}^H \right) \mathbf{g} \quad (8a)$$

$$\text{s.t. } \gamma_k \geq r_{k,\text{th}}, k \in \mathcal{K}, \quad (8b)$$

$$\gamma_{e,k} \leq r_{e,k,\text{th}}, k \in \mathcal{K}, \quad (8c)$$

$$\sum_{k=1}^K \|\mathbf{w}_{c,k}\|^2 + \sum_{n=1}^N \|\mathbf{w}_{r,n}\|^2 \leq P_{\max}, \quad (8d)$$

$$|v_m| = 1, m \in \mathcal{M}, \quad (8e)$$

where  $r_{k,\text{th}}$  in (8b) denotes the minimum SINR required by user  $k$ ,  $r_{e,k,\text{th}}$  in (8c) represents the maximum tolerable leakage of user  $k$ 's information to the target,  $P_{\max}$  in (8d) stands for the maximum allowed transmit power at the BS, and constraint (8e) denotes the unit-modulus constraint imposed on each IRS phase shift. Note that with constraints (8b) and (8c), the level of physical layer security of the ISAC system is guaranteed [38].

## 2) Imperfect CSI and Uncertain Target Location Scenario:

In this scenario, perfect CSI of the communication channels is not available at the BS, and the precise location of the target is unknown but the region of interest for sensing is available, i.e.,  $\Phi_h = [\theta - \Delta\theta, \theta + \Delta\theta]$  and  $\Phi_v = [\varphi - \Delta\varphi, \varphi + \Delta\varphi]$  are known, where  $\Delta\theta$  and  $\Delta\varphi$  represent the azimuth and vertical sensing range, respectively. Defining  $\mathbf{F}_k = \text{diag}(\mathbf{h}_{r,k}^H) \mathbf{G}$  and  $\mathbf{F}_r = \text{diag}(\mathbf{g}_r^H) \mathbf{G}$ , we can rewrite  $\mathbf{h}_k^H = \mathbf{h}_{r,k}^H \Theta \mathbf{G} + \mathbf{h}_{d,k}^H = \mathbf{v}^H \mathbf{F}_k + \mathbf{h}_{d,k}^H$  and  $\mathbf{g}^H = \mathbf{g}_r^H \Theta \mathbf{G} = \mathbf{v}^H \mathbf{F}_r$ , where  $\mathbf{v}^H = [v_1, \dots, v_M]$ . The bounded CSI error models for channels  $\mathbf{F}_k$ ,  $\mathbf{F}_r$ , and  $\mathbf{h}_{d,k}$  are respectively given by [39]<sup>2</sup>

$$\mathbf{F}_k = \hat{\mathbf{F}}_k + \Delta \mathbf{F}_k, \text{ with } \mathcal{F}_k = \{\Delta \mathbf{F}_k : \|\Delta \mathbf{F}_k\|_F \leq \varepsilon_k\}, \forall k, \quad (9)$$

$$\mathbf{F}_r = \hat{\mathbf{F}}_r + \Delta \mathbf{F}_r, \text{ with } \mathcal{F}_r = \{\Delta \mathbf{F}_r : \|\Delta \mathbf{F}_r\|_F \leq \varepsilon_r\}, \quad (10)$$

$$\mathbf{h}_{d,k} = \hat{\mathbf{h}}_{d,k} + \Delta \mathbf{h}_{d,k}, \text{ with } \mathcal{H}_{d,k} = \{\Delta \mathbf{h}_{d,k} : \|\Delta \mathbf{h}_{d,k}\| \leq \varepsilon_{d,k}\}, \forall k, \quad (11)$$

where  $\hat{\mathbf{G}}$  represents the estimated channel for the BS-IRS link,  $\hat{\mathbf{F}}_k$  denotes the estimated cascaded channel for user  $k$ ,  $\hat{\mathbf{F}}_r = \text{diag}(\mathbf{g}_r^H) \hat{\mathbf{G}}$  stands for the estimated cascaded channel for the target. Accordingly, the problem is formulated as<sup>3</sup>

$$\max_{\{\mathbf{w}_{c,k}, \mathbf{w}_{r,n}, v_m\}} \min_{\substack{\theta_h \in \Phi_h, \\ \varphi_v \in \Phi_v}} \mathbf{g}^H \left( \sum_{k=1}^K \mathbf{w}_{c,k} \mathbf{w}_{c,k}^H + \sum_{n=1}^N \mathbf{w}_{r,n} \mathbf{w}_{r,n}^H \right) \mathbf{g} \quad (12a)$$

$$\text{s.t. } \gamma_k \geq r_{k,\text{th}}, \Delta \mathbf{h}_{d,k} \in \mathcal{H}_{d,k}, \Delta \mathbf{F}_k \in \mathcal{F}_k, k \in \mathcal{K}, \quad (12b)$$

$$\gamma_{e,k} \leq r_{e,k,\text{th}}, \theta_h \in \Phi_h, \varphi_v \in \Phi_v, \Delta \mathbf{F}_r \in \mathcal{F}_r, k \in \mathcal{K}, \quad (12c)$$

$$\sum_{k=1}^K \|\mathbf{w}_{c,k}\|^2 + \sum_{n=1}^N \|\mathbf{w}_{r,n}\|^2 \leq P_{\max}, \quad (12d)$$

$$|v_m| = 1, m \in \mathcal{M}. \quad (12e)$$

The above two problems (8) and (12) are both non-convex due to the fact that the IRS reflection coefficients are constrained to be unit modulus, and because the optimization variables are coupled in both the objective functions and constraints. In general, there are no standard methods for solving such non-convex optimization problems optimally. In particular, (12b) and (12c) involve an infinite number of inequalities, which makes problem (12) even more difficult to address. In the following, we first propose a penalty-based algorithm for solving problem (8) in Section III and then propose an AO algorithm based on the  $\mathcal{S}$ -procedure and sign-definiteness approaches for solving problem (12) in Section IV.

### III. PROPOSED SOLUTION FOR PERFECT CSI AND KNOWN TARGET LOCATION

In this section, we consider the case where perfect CSI and target location are known at the BS, which provides a performance upper bound for the case with imperfect CSI and uncertain target location. To obtain a high-quality solution for problem (8), a penalty-based algorithm is proposed to decouple constraint coupling between the optimization variables in different blocks. Define auxiliary variables  $\{y_{c,k}, y_{r,n}, z_{c,k,i}, z_{r,k,n}, i \in \mathcal{K}, k \in \mathcal{K}, n \in \mathcal{N}\}$  and let

<sup>2</sup>The bounded CSI error models for  $\mathbf{F}_r$  and  $\mathbf{G}$  are equivalent since  $\mathbf{g}_r^H$  is a deterministic LoS channel. For notational simplicity, we use the bounded CSI error model for  $\mathbf{F}_r$  in the sequel.

<sup>3</sup>In this scenario, we drop the direction indices, i.e.,  $\theta_h$  and  $\varphi_v$ , and use the notation  $\mathbf{g}$  to represent  $\mathbf{g}(\theta_h, \varphi_v)$  for the brevity.

$\mathbf{g}^H \mathbf{w}_{c,k} = y_{c,k}$ ,  $\mathbf{g}^H \mathbf{w}_{r,n} = y_{r,n}$ ,  $\mathbf{h}_k^H \mathbf{w}_{c,i} = z_{c,k,i}$ , and  $\mathbf{h}_k^H \mathbf{w}_{r,n} = z_{r,k,n}$ . Problem (8) can be equivalently transformed as

$$\max_{\{\mathbf{w}_{c,k}, \mathbf{w}_{r,n}, \{v_m\}, \Omega\}} \sum_{k=1}^K |y_{c,k}|^2 + \sum_{n=1}^N |y_{r,n}|^2 \quad (13a)$$

$$\text{s.t. } \frac{|z_{c,k,k}|^2}{\sum_{i \neq k}^K |z_{c,k,i}|^2 + \sum_{n=1}^N |z_{r,k,n}|^2 + \sigma_k^2} \geq r_{k,\text{th}}, k \in \mathcal{K}, \quad (13b)$$

$$\frac{|y_{c,k}|^2}{\sum_{i \neq k}^K |y_{c,i}|^2 + \sum_{n=1}^N |y_{r,n}|^2 + \sigma_i^2} \leq r_{e,k,\text{th}}, k \in \mathcal{K}, \quad (13c)$$

$$\mathbf{g}^H \mathbf{w}_{c,k} = y_{c,k}, \mathbf{g}^H \mathbf{w}_{r,n} = y_{r,n}, \mathbf{h}_k^H \mathbf{w}_{c,k} = z_{c,k,i}, \quad (13d)$$

$$\mathbf{h}_k^H \mathbf{w}_{r,n} = z_{r,k,n}, i \in \mathcal{K}, k \in \mathcal{K}, n \in \mathcal{N}, \quad (13e)$$

where  $\Omega = \{y_{c,k}, y_{r,n}, z_{c,k,i}, z_{r,k,n}\}$ . We then reformulate (13d) as penalty terms that are added to the objective function (13a) yielding the following optimization problem

$$\max_{\{\mathbf{w}_{c,k}, \mathbf{w}_{r,n}, v_m\}, \Omega} \sum_{k=1}^K |y_{c,k}|^2 + \sum_{n=1}^N |y_{r,n}|^2 - \frac{1}{2\rho} \times \left( \sum_{k=1}^K |\mathbf{g}^H \mathbf{w}_{c,k} - y_{c,k}|^2 + \sum_{n=1}^N |\mathbf{g}^H \mathbf{w}_{r,n} - y_{r,n}|^2 + \sum_{k=1}^K \sum_{i=1}^K |\mathbf{h}_k^H \mathbf{w}_{c,i} - z_{c,k,i}|^2 + \sum_{k=1}^K \sum_{n=1}^N |\mathbf{h}_k^H \mathbf{w}_{r,n} - z_{r,k,n}|^2 \right) \quad (14a)$$

$$\text{s.t. } (8d), (8e), (13b), (13c), \quad (14b)$$

where  $\rho > 0$  represents the parameter that penalizes the violations of the equality constraints in (13d). To address problem (14), a penalty-based algorithm comprising two layers is proposed, where in the outer layer, we gradually update the penalty parameter, while in the inner loop, we alternately optimize the variables in different blocks.

#### A. Inner Layer Optimization

In the inner layer, we divide all the optimization variables into three blocks: 1) auxiliary variable set  $\Omega$ , 2) transmit beamformers  $\{\mathbf{w}_{c,k}, \mathbf{w}_{r,n}\}$ , and 3) IRS phase shifts  $\{v_m\}$ .

1) *Optimizing  $\Omega$  for given  $\{\mathbf{w}_{c,k}, \mathbf{w}_{r,n}\}$  and  $\{v_m\}$* : This subproblem can be written as

$$\max_{\Omega} \sum_{k=1}^K |y_{c,k}|^2 + \sum_{n=1}^N |y_{r,n}|^2 - \frac{1}{2\rho} \times \left( \sum_{k=1}^K |\mathbf{g}^H \mathbf{w}_{c,k} - y_{c,k}|^2 + \sum_{n=1}^N |\mathbf{g}^H \mathbf{w}_{r,n} - y_{r,n}|^2 + \sum_{k=1}^K \sum_{i=1}^K |\mathbf{h}_k^H \mathbf{w}_{c,i} - z_{c,k,i}|^2 + \sum_{k=1}^K \sum_{n=1}^N |\mathbf{h}_k^H \mathbf{w}_{r,n} - z_{r,k,n}|^2 \right) \quad (15a)$$

$$\text{s.t. } (13b), (13c). \quad (15b)$$

Since the optimization variables with respect to (w.r.t.) different blocks  $\{y_{c,k}, y_{r,n}, \forall k, \forall n\}$  and  $\{z_{c,k,i}, z_{r,k,n}, \forall i, \forall n\}$  for  $k \in \mathcal{K}$  are separable in both the objective function and constraints, we can independently solve  $K+1$  subproblems in parallel. Specifically, the subproblem corresponding to the  $k$ th block  $\{z_{c,k,i}, z_{r,k,n}, \forall i, \forall n\}$  is given by

$$\min_{\substack{z_{c,k,i}, \\ z_{r,k,n}}} \sum_{i=1}^K |\mathbf{h}_k^H \mathbf{w}_{c,i} - z_{c,k,i}|^2 + \sum_{n=1}^N |\mathbf{h}_k^H \mathbf{w}_{r,n} - z_{r,k,n}|^2 \quad (16a)$$

$$\text{s.t. } \frac{|z_{c,k,k}|^2}{\sum_{i \neq k}^K |z_{c,k,i}|^2 + \sum_{n=1}^N |z_{r,k,n}|^2 + \sigma_k^2} \geq r_{k,\text{th}}. \quad (16b)$$

It is not difficult to see that problem (16) is a quadratically constrained quadratic program (QCQP) with a convex objective function and non-convex constraint (16b). Fortunately, it was shown in [40, Appendix B.1] that strong duality holds for any optimization problem with a quadratic objective and one quadratic inequality constraint, provided that the Slater's condition holds. Therefore, we can solve problem (16) by solving its dual problem. Specifically, by introducing dual variable  $\mu_1 \geq 0$  associated with constraint (16b), the Lagrangian function of problem (16) is given by

$$\begin{aligned} \mathcal{L}_1(z_{c,k,i}, z_{r,k,n}, \mu_1) = & \sum_{i=1}^K |\mathbf{h}_k^H \mathbf{w}_{c,k} - z_{c,k,i}|^2 + \sum_{n=1}^N |\mathbf{h}_k^H \mathbf{w}_{r,n} - z_{r,k,n}|^2 + \mu_1 \times \\ & \left( r_{k,\text{th}} \left( \sum_{i \neq k}^K |z_{c,k,i}|^2 + \sum_{n=1}^N |z_{r,k,n}|^2 + \sigma_k^2 \right) - |z_{c,k,k}|^2 \right). \end{aligned} \quad (17)$$

Accordingly, the corresponding dual function is given by  $\min_{z_{c,k,i}, z_{r,k,n}} \mathcal{L}_1(z_{c,k,i}, z_{r,k,n}, \mu_1)$ . It can be readily checked that to make the dual function bounded, we must have  $0 \leq \mu_1 < 1$ . Taking the first-order derivative of  $\mathcal{L}_1(z_{c,k,i}, z_{r,k,n}, \mu_1)$  w.r.t.  $z_{c,k,i}$  and  $z_{r,k,n}$  and setting both to zero, we obtain the optimal solution as

$$z_{c,k,i}^{\text{opt}}(\mu_1) = \begin{cases} \frac{\mathbf{h}_k^H \mathbf{w}_{c,i}}{1 + \mu_1 r_{k,\text{th}}}, & i \neq k, i \in \mathcal{K}, \\ \frac{\mathbf{h}_k^H \mathbf{w}_{c,k}}{1 - \mu_1}, & i = k, \end{cases} \quad (18)$$

$$z_{r,k,n}^{\text{opt}}(\mu_1) = \frac{\mathbf{h}_k^H \mathbf{w}_{r,n}}{1 + \mu_1 r_{k,\text{th}}}, \quad n \in \mathcal{N}. \quad (19)$$

If constraint (16b) is not met with equality at the optimal solution, i.e.,  $\mu_1^{\text{opt}} = 0$ , then the optimal solutions to problem (16) are given by  $z_{c,k,i}^{\text{opt}}(0)$  and  $z_{r,k,n}^{\text{opt}}(0)$ . Otherwise, the optimal  $\mu_1^{\text{opt}}$  is a positive value ( $0 < \mu_1^{\text{opt}} < 1$ ) that satisfies the equality constraint (16b), i.e.,

$$\begin{aligned} r_{k,\text{th}} \left( \sum_{i \neq k}^K |z_{c,k,i}^{\text{opt}}(\mu_1^{\text{opt}})|^2 + \sum_{n=1}^N |z_{r,k,n}^{\text{opt}}(\mu_1^{\text{opt}})|^2 + \sigma_k^2 \right) \\ - |z_{c,k,k}^{\text{opt}}(\mu_1^{\text{opt}})|^2 = 0. \end{aligned} \quad (20)$$

It can be readily verified that  $|z_{c,k,i}^{\text{opt}}(\mu_1)|^2$  for  $i \neq k$  and  $z_{r,k,n}^{\text{opt}}(\mu_1)$  are both monotonically decreasing with  $\mu_1$ , while  $z_{c,k,k}^{\text{opt}}(\mu_1)$  is monotonically increasing with  $\mu_1$  for  $0 < \mu_1 < 1$ . As such, the optimal  $\mu_1^{\text{opt}}$  can be obtained by applying a simple bisection search method between 0 and 1.

The subproblem corresponding to block  $\{y_{c,k}, y_{r,n}, \forall k, \forall n\}$  is given by

$$\begin{aligned} \max_{\{y_{c,k}, y_{r,n}\}} \sum_{k=1}^K |y_{c,k}|^2 + \sum_{n=1}^N |y_{r,n}|^2 - \frac{1}{2\rho} \left( \sum_{k=1}^K |\mathbf{g}^H \mathbf{w}_{c,k} - y_{c,k}|^2 \right. \\ \left. + \sum_{n=1}^N |\mathbf{g}^H \mathbf{w}_{r,n} - y_{r,n}|^2 \right) \end{aligned} \quad (21a)$$

$$\text{s.t. (13c)}. \quad (21b)$$

It is observed that the objective function (21a) is a difference of two convex (DC) functions, which is non-convex. To solve it, the successive convex approximation (SCA) technique is applied. Specifically, for any given points  $y_{c,k}^r$  and  $y_{r,n}^r$ , we have

$$|y_{c,k}|^2 \geq -|y_{c,k}^r|^2 + 2\text{Re}\{y_{c,k}^H y_{c,k}^r\} \triangleq f_1^{\text{lb}}(y_{c,k}), \quad \forall k, \quad (22)$$

$$|y_{r,n}|^2 \geq -|y_{r,n}^r|^2 + 2\text{Re}\{y_{r,n}^H y_{r,n}^r\} \triangleq f_2^{\text{lb}}(y_{r,n}), \quad \forall n. \quad (23)$$

As a result, problem (21) can be approximated as

$$\begin{aligned} \max_{\{y_{c,k}, y_{r,n}\}} \sum_{k=1}^K f_1^{\text{lb}}(y_{c,k}) + \sum_{n=1}^N f_2^{\text{lb}}(y_{r,n}) - \frac{1}{2\rho} \times \\ \sum_{k=1}^K |\mathbf{g}^H \mathbf{w}_{c,k} - y_{c,k}|^2 + \sum_{n=1}^N |\mathbf{g}^H \mathbf{w}_{r,n} - y_{r,n}|^2 \quad (24a) \\ \text{s.t. } |y_{c,k}|^2 \leq r_{e,k,\text{th}} \left( \sum_{i \neq k}^K f_1^{\text{lb}}(y_{c,i}) + \sum_{n=1}^N f_2^{\text{lb}}(y_{r,n}) + \sigma_k^2 \right), \quad \forall k. \end{aligned} \quad (24b)$$

It can be readily seen that problem (24) is a QCQP, which can be optimally solved by the interior-point method [40].

2) *Optimizing  $\{\mathbf{w}_{c,k}, \mathbf{w}_{r,n}\}$  for given  $\{v_m\}$  and  $\Omega$* : This subproblem is given by (dropping irrelevant constants w.r.t.  $\{\mathbf{w}_{c,k}, \mathbf{w}_{r,n}\}$ )

$$\begin{aligned} \min_{\{\mathbf{w}_{c,k}, \{\mathbf{w}_{r,n}\}} \sum_{k=1}^K |\mathbf{g}^H \mathbf{w}_{c,k} - y_{c,k}|^2 + \sum_{n=1}^N |\mathbf{g}^H \mathbf{w}_{r,n} - y_{r,n}|^2 + \\ \sum_{k=1}^K \sum_{i=1}^K |\mathbf{h}_k^H \mathbf{w}_{c,i} - z_{c,k,i}|^2 + \sum_{k=1}^K \sum_{n=1}^N |\mathbf{h}_k^H \mathbf{w}_{r,n} - z_{r,k,n}|^2 \end{aligned} \quad (25a)$$

$$\text{s.t. (8d)}. \quad (25b)$$

Note that problem (25) is also a QCQP, which can be solved by the interior point method but with a high computational complexity [40]. To reduce the computational complexity, we obtain a semi-closed-form yet optimal solution for the transmit beamformers by using the Lagrange duality method. By introducing the dual variable  $\mu_2 \geq 0$  associated with constraint (8d), the Lagrangian function of problem (25) is given by

$$\begin{aligned} \mathcal{L}_2(\mathbf{w}_{c,k}, \mathbf{w}_{r,n}, \mu_2) = \sum_{k=1}^K |\mathbf{g}^H \mathbf{w}_{c,k} - y_{c,k}|^2 + \sum_{n=1}^N |\mathbf{g}^H \mathbf{w}_{r,n} - y_{r,n}|^2 \\ + \sum_{k=1}^K \sum_{i=1}^K |\mathbf{h}_k^H \mathbf{w}_{c,i} - z_{c,k,i}|^2 + \sum_{k=1}^K \sum_{n=1}^N |\mathbf{h}_k^H \mathbf{w}_{r,n} - z_{r,k,n}|^2 + \\ \mu_2 \left( \sum_{k=1}^K \|\mathbf{w}_{c,k}\|^2 + \sum_{n=1}^N \|\mathbf{w}_{r,n}\|^2 - P_{\text{max}} \right). \end{aligned} \quad (26)$$

By taking the first-order derivative of  $\mathcal{L}_2(\mathbf{w}_{c,k}, \mathbf{w}_{r,n}, \mu_2)$  w.r.t.  $\mathbf{w}_{c,k}$  and  $\mathbf{w}_{r,n}$  and setting both to zero, we obtain the optimal solutions as

$$\begin{aligned} \mathbf{w}_{c,k}^{\text{opt}}(\mu_2) = \left( \mathbf{g}\mathbf{g}^H + \sum_{i=1}^K \mathbf{h}_i \mathbf{h}_i^H + \mu_2 \mathbf{I}_N \right)^{-1} \\ \times \left( y_{c,k} \mathbf{g} + \sum_{i=1}^K z_{c,i,k} \mathbf{h}_i \right), \quad k \in \mathcal{K}, \end{aligned} \quad (27)$$

$$\begin{aligned} \mathbf{w}_{r,n}^{\text{opt}}(\mu_2) = \left( \mathbf{g}\mathbf{g}^H + \sum_{i=1}^K \mathbf{h}_i \mathbf{h}_i^H + \mu_2 \mathbf{I}_N \right)^{-1} \\ \times \left( y_{r,n} \mathbf{g} + \sum_{i=1}^K z_{r,i,n} \mathbf{h}_i \right), \quad n \in \mathcal{N}. \end{aligned} \quad (28)$$

Note that the optimal solution must be satisfied with the following complementary slackness condition [40]

$$\mu_2^{\text{opt}} (P(\mu_2^{\text{opt}}) - P_{\text{max}}) = 0, \quad (29)$$

where  $P(\mu_1^{\text{opt}}) = \sum_{k=1}^K \|\mathbf{w}_{c,k}^{\text{opt}}(\mu_1^{\text{opt}})\|^2 + \sum_{n=1}^N \|\mathbf{w}_{r,n}^{\text{opt}}(\mu_1^{\text{opt}})\|^2$ .

We first check whether  $\mu_2^{\text{opt}} = 0$  is the optimal solution or not. If  $P(0) - P_{\text{max}} < 0$ , it means that the optimal dual variable  $\mu_2^{\text{opt}}$  equals 0; otherwise, the optimal  $\mu_2^{\text{opt}}$  is a positive value that satisfies  $P(\mu_2^{\text{opt}}) - P_{\text{max}} = 0$ , and can be obtained as

follows. Let  $\mathbf{S} = \mathbf{g}\mathbf{g}^H + \sum_{i=1}^K \mathbf{h}_i \mathbf{h}_i^H$ ,  $\mathbf{t}_{c,k} = y_{c,k} \mathbf{g} + \sum_{i=1}^K z_{c,i,k} \mathbf{h}_i$ ,

and  $\mathbf{t}_{r,n} = y_{r,n} \mathbf{g} + \sum_{i=1}^K z_{r,i,n} \mathbf{h}_i$ , which implies

$$\begin{aligned} \left\| \mathbf{w}_{c,k}^{\text{opt}}(\mu_2) \right\|^2 &= \text{tr} \left( (\mathbf{S} + \mu_2 \mathbf{I}_N)^{-2} \mathbf{t}_{c,k} \mathbf{t}_{c,k}^H \right), \\ \left\| \mathbf{w}_{r,n}^{\text{opt}}(\mu_2) \right\|^2 &= \text{tr} \left( (\mathbf{S} + \mu_2 \mathbf{I}_N)^{-2} \mathbf{t}_{r,n} \mathbf{t}_{r,n}^H \right). \end{aligned} \quad (30)$$

Since  $\mathbf{S}$  is a positive semi-definite matrix, its eigendecomposition can be expressed as  $\mathbf{S} = \mathbf{U}\mathbf{\Sigma}\mathbf{U}^H$ . Substituting it into (30) yields

$$P(\mu_2) = \sum_{i=1}^N \frac{\left( \mathbf{U}^H \left( \sum_{k=1}^K \mathbf{t}_{c,k} \mathbf{t}_{c,k}^H + \sum_{n=1}^N \mathbf{t}_{r,n} \mathbf{t}_{r,n}^H \right) \mathbf{U} \right)_{i,i}}{(\mathbf{\Sigma}_{i,i} + \mu_2)^2}. \quad (31)$$

It can be readily seen that  $P(\mu_2)$  is monotonically decreasing w.r.t.  $\mu_2$ , which motivates us to apply the bisection method to search for  $\mu_2$  satisfying  $P(\mu_2^{\text{opt}}) = P_{\max}$ . To reduce the search space, an upper bound of  $\mu_2$  can be derived as

$$\mu_2^{\text{up}} = \sqrt{\sum_{i=1}^N \left( \mathbf{U}^H \left( \sum_{k=1}^K \mathbf{t}_{c,k} \mathbf{t}_{c,k}^H + \sum_{n=1}^N \mathbf{t}_{r,n} \mathbf{t}_{r,n}^H \right) \mathbf{U} \right)_{i,i}} / P_{\max}$$

by setting  $\mathbf{\Sigma}_{i,i}$  in (31) to zero.

3) *Optimizing  $\{v_m\}$  for given  $\{\mathbf{w}_{c,k}, \mathbf{w}_{r,n}\}$  and  $\Omega$* : This subproblem is given by (ignoring the constant terms w.r.t.  $\{v_m\}$ )

$$\begin{aligned} \min_{\{v_m\}} & \sum_{k=1}^K \left| \mathbf{g}^H \mathbf{w}_{c,k} - y_{c,k} \right|^2 + \sum_{n=1}^N \left| \mathbf{g}^H \mathbf{w}_{r,n} - y_{r,n} \right|^2 + \\ & \sum_{k=1}^K \sum_{i=1}^K \left| \mathbf{h}_k^H \mathbf{w}_{c,i} - z_{c,k,i} \right|^2 + \sum_{k=1}^K \sum_{n=1}^N \left| \mathbf{h}_k^H \mathbf{w}_{r,n} - z_{r,k,n} \right|^2 \quad (32a) \\ \text{s.t.} & \quad (8e). \quad (32b) \end{aligned}$$

Although the objective function (32a) is a quadratic function of  $\mathbf{v}$ , the unit-modulus constraint imposed on each IRS phase shift in (8e) is non-convex. Here, we construct an upper-bounded convex surrogate function for (32a) by applying the MM algorithm [41], based on which a closed-form solution for the IRS phase shifts is derived. Specifically, the surrogate function at any given point  $\mathbf{v}^r$ , denoted by  $\varpi(\mathbf{v}|\mathbf{v}^r)$ , for a quadratic function  $\mathbf{v}^H \mathbf{A} \mathbf{v}$  can be expressed as

$$\begin{aligned} \varpi(\mathbf{v}|\mathbf{v}^r) &= \lambda_{\max} \mathbf{v}^H \mathbf{v} - 2\text{Re} \left\{ \mathbf{v}^H (\lambda_{\max} \mathbf{I}_M - \mathbf{A}) \mathbf{v}^r \right\} \\ &+ \mathbf{v}^{r,H} (\lambda_{\max} \mathbf{I}_M - \mathbf{A}) \mathbf{v}^r, \end{aligned} \quad (33)$$

where  $\mathbf{A} \in \mathbb{C}^{M \times M}$  is positive semi-definite, and  $\lambda_{\max}$  is the maximum eigenvalue of  $\mathbf{A}$ . As a result, based on  $\mathbf{v}^H \mathbf{v} = M$ , we can solve the following approximate optimization problem (ignoring constant terms w.r.t.  $\{v_m\}$ )

$$\begin{aligned} \max_{v_m} & \text{Re} \left\{ \mathbf{v}^H \mathbf{q}^r \right\} \quad (34a) \\ \text{s.t.} & \quad (8e), \quad (34b) \end{aligned}$$

$$\begin{aligned} \text{where } \mathbf{q}^r &= \sum_{k=1}^K \left( (\lambda_{\max,1,k} \mathbf{I}_M - \Upsilon_{r,c,k}) \mathbf{v}^r + y_{c,k}^H \mathbf{F}_r \mathbf{w}_{c,k} \right) \\ &+ \sum_{n=1}^N \left( (\lambda_{\max,2,n} \mathbf{I}_M - \Upsilon_{r,r,n}) \mathbf{v}^r + y_{r,n}^H \mathbf{F}_r \mathbf{w}_{r,n} \right) \\ &+ \sum_{k=1}^K \sum_{i=1}^K \left( (\lambda_{\max,3,k} \mathbf{I}_M - \Upsilon_{c,k,i}) \mathbf{v}^r - \Psi_{c,k,i} \right) \\ &+ \sum_{k=1}^K \sum_{n=1}^N \left( (\lambda_{\max,4,k,n} \mathbf{I}_M - \Upsilon_{r,k,n}) \mathbf{v}^r - \Psi_{r,n,k} \right), \\ \Psi_{c,k,i} &= \mathbf{F}_k \mathbf{w}_{c,i} \left( \mathbf{w}_{c,i}^H \mathbf{h}_{d,k} - z_{c,k,i}^H \right), \quad \Psi_{r,n,k} = \\ &\mathbf{F}_k \mathbf{w}_{r,n} \left( \mathbf{w}_{r,n}^H \mathbf{h}_{d,k} - z_{r,k,n}^H \right), \quad \Upsilon_{r,c,k} = \mathbf{F}_r \mathbf{w}_{c,k} \mathbf{w}_{c,k}^H \mathbf{F}_r^H, \end{aligned}$$

**Algorithm 1** Penalty-based algorithm for solving problem (8).

- 1: **Initialize**  $\mathbf{v}$ ,  $\{\mathbf{w}_{c,k}, \mathbf{w}_{r,n}\}$ ,  $\{y_{c,k}, y_{r,n}\}$ ,  $c$ ,  $\rho$ ,  $\varepsilon_{\text{in}}$ , and  $\varepsilon_{\text{out}}$ .
- 2: **repeat: outer layer**
- 3:   **repeat: inner layer**
- 4:     Update auxiliary variables  $\{z_{c,k,i}, z_{r,k,n}\}$  by solving problem (16).
- 5:     Update auxiliary variables  $\{y_{c,k}, y_{r,n}\}$  by solving problem (24).
- 6:     Update transmit beamformers  $\{\mathbf{w}_{c,k}, \mathbf{w}_{r,n}\}$  by solving problem (25).
- 7:     Update IRS phase shifts  $\{v_m\}$  based on (35).
- 8:   **until** the fractional increase of the objective value of (14) is below a threshold  $\varepsilon_{\text{in}}$ .
- 9:   Update penalty parameter  $\rho$  based on (36).
- 10: **until** termination indicator  $\xi$  defined in (37) is below a threshold  $\varepsilon_{\text{out}}$ .

$\Upsilon_{r,r,n} = \mathbf{F}_r \mathbf{w}_{r,n} \mathbf{w}_{r,n}^H \mathbf{F}_r^H$ ,  $\Upsilon_{c,k,i} = \mathbf{F}_k \mathbf{w}_{c,i} \mathbf{w}_{c,i}^H \mathbf{F}_k^H$ ,  $\Upsilon_{r,k,n} = \mathbf{F}_k \mathbf{w}_{r,n} \mathbf{w}_{r,n}^H \mathbf{F}_k^H$ , and  $\lambda_{\max,1,k}$ ,  $\lambda_{\max,2,n}$ ,  $\lambda_{\max,3,k,i}$ , and  $\lambda_{\max,4,k,n}$  represent the maximum eigenvalues of  $\Upsilon_{r,c,k}$ ,  $\Upsilon_{r,r,n}$ ,  $\Upsilon_{c,k,i}$ , and  $\Upsilon_{r,k,n}$ , respectively. The optimal solution  $\mathbf{v}$  to problem (34) is then given by

$$\mathbf{v}^{\text{opt}} = e^{j \arg(\mathbf{q}^r)}. \quad (35)$$

## B. Outer Layer Optimization

In the outer layer, the penalty parameter in the  $r$ th iteration is updated as follows

$$\rho^r = c\rho^{r-1}, \quad 0 < c < 1, \quad (36)$$

where  $c$  is a constant scaling factor that is used to control the convergence behavior.

## C. Overall Algorithm and Computational Complexity

The termination indicator for the penalty-based algorithm is given by

$$\begin{aligned} \xi &= \max_{i,k,n} \left\{ \left| \mathbf{g}^H \mathbf{w}_{c,k} - y_{c,k} \right|^2, \left| \mathbf{g}^H \mathbf{w}_{r,n} - y_{r,n} \right|^2, \right. \\ &\left. \left| \mathbf{h}_k^H \mathbf{w}_{c,i} - z_{c,k,i} \right|^2, \left| \mathbf{h}_k^H \mathbf{w}_{r,n} - z_{r,k,n} \right|^2 \right\}. \end{aligned} \quad (37)$$

If  $\xi$  is smaller than a predefined value, constraint (13d) is considered to be met with equality for a given accuracy. The proposed algorithm is summarized in Algorithm 1, whose computational complexity is given by  $\mathcal{O}(I_{\text{out}} I_{\text{in}} (K \log_2(\frac{1}{\varepsilon}) N^3 + \log_2(\frac{\mu_2^{\text{up}}}{\varepsilon}) N^3 + (K+N)^{3.5} + M^3))$ , where  $\varepsilon$  represents the iteration accuracy, and  $I_{\text{in}}$  and  $I_{\text{out}}$  denote the numbers of iterations required for reaching convergence in the inner layer and outer layer, respectively.

## IV. PROPOSED SOLUTION FOR IMPERFECT CSI AND UNCERTAIN TARGET LOCATION

In this section, we consider the case with imperfect CSI and uncertain target location. Since problem (12) involves an infinite number of inequalities in constraints (12b) and (12c), the previous penalty-based algorithm is no longer applicable for solving problem (12), which thus calls for new algorithm design. By introducing auxiliary variables  $\{\beta_{c,k} \geq 0\}$  satisfying

$\beta_{c,k} = \sum_{i \neq k}^K |\mathbf{h}_k^H \mathbf{w}_{c,i}|^2 + \sum_{n=1}^N |\mathbf{h}_k^H \mathbf{w}_{r,n}|^2 + \sigma_k^2$ ,  $k \in \mathcal{K}$ , constraint (12b) can be equivalently transformed as

$$|\mathbf{h}_k^H \mathbf{w}_{c,k}|^2 \geq \beta_{c,k} r_{k,\text{th}}, \Delta \mathbf{h}_{d,k} \in \mathcal{H}_{d,k}, \Delta \mathbf{F}_k \in \mathcal{F}_k, k \in \mathcal{K}, \quad (38)$$

$$\sum_{i \neq k}^K |\mathbf{h}_k^H \mathbf{w}_{c,i}|^2 + \sum_{n=1}^N |\mathbf{h}_k^H \mathbf{w}_{r,n}|^2 + \sigma_k^2 \leq \beta_{c,k}, \Delta \mathbf{h}_{d,k} \in \mathcal{H}_{d,k}, \Delta \mathbf{F}_k \in \mathcal{F}_k, k \in \mathcal{K}. \quad (39)$$

Although the left-hand side of (38) is convex w.r.t  $\mathbf{v}$  (recall that  $\mathbf{h}_k^H = \mathbf{v}^H \mathbf{F}_k + \mathbf{h}_{d,k}^H$ ), the resulting set is not a convex set since the superlevel set of a convex quadratic function is not convex in general. To address this non-convex constraint, we take the first-order Taylor expansion of  $|\mathbf{h}_k^H \mathbf{w}_{c,k}|^2$  at any given feasible point  $\mathbf{v}^r$  to obtain the following lower bound

$$|\mathbf{h}_k^H \mathbf{w}_{c,k}|^2 \geq f_k^{\text{lb}}(\mathbf{v}) \triangleq -|\mathbf{v}^{r,H} \mathbf{F}_k \mathbf{w}_{c,k}^r + \mathbf{h}_{d,k}^H \mathbf{w}_{c,k}^r|^2 + 2\text{Re}\left\{ (\mathbf{v}^H \mathbf{F}_k \mathbf{w}_{c,k} + \mathbf{h}_{d,k}^H \mathbf{w}_{c,k})^H (\mathbf{v}^{r,H} \mathbf{F}_k \mathbf{w}_{c,k}^r + \mathbf{h}_{d,k}^H \mathbf{w}_{c,k}^r) \right\} \quad (40)$$

which is linear and convex w.r.t  $\mathbf{v}$ .

Substituting  $\mathbf{F}_k = \hat{\mathbf{F}}_k + \Delta \mathbf{F}_k$  and  $\mathbf{h}_{d,k} = \hat{\mathbf{h}}_{d,k} + \Delta \mathbf{h}_{d,k}$  into term  $|\mathbf{v}^{r,H} \mathbf{F}_k \mathbf{w}_{c,k}^r + \mathbf{h}_{d,k}^H \mathbf{w}_{c,k}^r|^2$  in (40), we can rewrite it as

$$\begin{aligned} & |\mathbf{v}^{r,H} \mathbf{F}_k \mathbf{w}_{c,k}^r + \mathbf{h}_{d,k}^H \mathbf{w}_{c,k}^r|^2 = \left| \hat{\mathbf{h}}_k^{r,H} \mathbf{w}_{c,k}^r \right|^2 + \\ & 2\text{Re}\left\{ \left( \hat{\mathbf{h}}_k^{r,H} \mathbf{w}_{c,k}^r \right)^H (\mathbf{v}^{r,H} \Delta \mathbf{F}_k \mathbf{w}_{c,k}^r + \Delta \mathbf{h}_{d,k}^H \mathbf{w}_{c,k}^r) \right\} + \\ & \left| \mathbf{v}^{r,H} \Delta \mathbf{F}_k \mathbf{w}_{c,k}^r + \Delta \mathbf{h}_{d,k}^H \mathbf{w}_{c,k}^r \right|^2, \end{aligned} \quad (41)$$

where  $\hat{\mathbf{h}}_k^{r,H} = \mathbf{v}^{r,H} \hat{\mathbf{F}}_k + \hat{\mathbf{h}}_{d,k}^H$ . Below, we rewrite terms in (41) into a compact form that facilitates the algorithm design. Specifically, we first expand  $|\mathbf{v}^{r,H} \Delta \mathbf{F}_k \mathbf{w}_{c,k}^r + \Delta \mathbf{h}_{d,k}^H \mathbf{w}_{c,k}^r|^2$  as

$$\begin{aligned} & \left| \mathbf{v}^{r,H} \Delta \mathbf{F}_k \mathbf{w}_{c,k}^r + \Delta \mathbf{h}_{d,k}^H \mathbf{w}_{c,k}^r \right|^2 = \mathbf{v}^{r,H} \Delta \mathbf{F}_k \mathbf{w}_{c,k}^r \mathbf{w}_{c,k}^{r,H} \Delta \mathbf{F}_k^H \mathbf{v}^r + \\ & \Delta \mathbf{h}_{d,k}^H \mathbf{w}_{c,k}^r \mathbf{w}_{c,k}^{r,H} \Delta \mathbf{h}_{d,k} + \mathbf{v}^{r,H} \Delta \mathbf{F}_k \mathbf{w}_{c,k}^r \mathbf{w}_{c,k}^{r,H} \Delta \mathbf{h}_{d,k} + \\ & \Delta \mathbf{h}_{d,k}^H \mathbf{w}_{c,k}^r \mathbf{w}_{c,k}^{r,H} \Delta \mathbf{F}_k^H \mathbf{v}^r, \end{aligned} \quad (42)$$

where

$$\begin{aligned} & \mathbf{v}^{r,H} \Delta \mathbf{F}_k \mathbf{w}_{c,k}^r \mathbf{w}_{c,k}^{r,H} \Delta \mathbf{F}_k^H \mathbf{v}^r = \\ & \text{vec}^H(\Delta \mathbf{F}_k^*) \left( \mathbf{w}_{c,k}^r \mathbf{w}_{c,k}^{r,H} \right) \otimes (\mathbf{v}^{r,*} \mathbf{v}^{r,T}) \text{vec}(\Delta \mathbf{F}_k^*), \end{aligned} \quad (43)$$

$$\begin{aligned} & \mathbf{v}^{r,H} \Delta \mathbf{F}_k \mathbf{w}_{c,k}^r \mathbf{w}_{c,k}^{r,H} \Delta \mathbf{h}_{d,k} = \\ & \text{vec}^H(\Delta \mathbf{F}_k^*) \left( \left( \mathbf{w}_{c,k}^r \mathbf{w}_{c,k}^{r,H} \right) \otimes \mathbf{v}^{r,*} \right) \Delta \mathbf{h}_{d,k}, \end{aligned} \quad (44)$$

$$\begin{aligned} & \Delta \mathbf{h}_{d,k}^H \mathbf{w}_{c,k}^r \mathbf{w}_{c,k}^{r,H} \Delta \mathbf{F}_k^H \mathbf{v}^r = \\ & \Delta \mathbf{h}_{d,k}^H \left( \left( \mathbf{w}_{c,k}^r \mathbf{w}_{c,k}^{r,H} \right) \otimes \mathbf{v}^{r,T} \right) \text{vec}(\Delta \mathbf{F}_k^*). \end{aligned} \quad (45)$$

Thus, we can rewrite  $|\mathbf{v}^{r,H} \Delta \mathbf{F}_k \mathbf{w}_{c,k}^r + \Delta \mathbf{h}_{d,k}^H \mathbf{w}_{c,k}^r|^2$  in a more compact form given by

$$\left| \mathbf{v}^{r,H} \Delta \mathbf{F}_k \mathbf{w}_{c,k}^r + \Delta \mathbf{h}_{d,k}^H \mathbf{w}_{c,k}^r \right|^2 = \Delta \mathbf{h}_{k,\text{eff}}^H \mathbf{H}_{c,k}^r \Delta \mathbf{h}_{k,\text{eff}}, \quad (46)$$

where  $\Delta \mathbf{h}_{k,\text{eff}}^H = \left[ \Delta \mathbf{h}_{d,k}^H \text{vec}^H(\Delta \mathbf{F}_k^*) \right]$ ,  $\mathbf{H}_{c,k}^r = \begin{bmatrix} \mathbf{w}_{c,k}^r \mathbf{w}_{c,k}^{r,H} & \left( \mathbf{w}_{c,k}^r \mathbf{w}_{c,k}^{r,H} \right) \otimes \mathbf{v}^{r,T} \\ \left( \mathbf{w}_{c,k}^r \mathbf{w}_{c,k}^{r,H} \right) \otimes \mathbf{v}^{r,*} & \left( \mathbf{w}_{c,k}^r \mathbf{w}_{c,k}^{r,H} \right) \otimes (\mathbf{v}^{r,*} \mathbf{v}^{r,T}) \end{bmatrix}$ . Then,

$\left( \hat{\mathbf{h}}_k^{r,H} \mathbf{w}_{c,k}^r \right)^H \left( \mathbf{v}^{r,H} \Delta \mathbf{F}_k \mathbf{w}_{c,k}^r + \Delta \mathbf{h}_{d,k}^H \mathbf{w}_{c,k}^r \right)$  can be expressed as

$$\begin{aligned} & \left( \hat{\mathbf{h}}_k^{r,H} \mathbf{w}_{c,k}^r \right)^H \left( \mathbf{v}^{r,H} \Delta \mathbf{F}_k \mathbf{w}_{c,k}^r + \Delta \mathbf{h}_{d,k}^H \mathbf{w}_{c,k}^r \right) = \\ & \left( \hat{\mathbf{h}}_k^{r,H} \mathbf{w}_{c,k}^r \right)^H \Delta \mathbf{h}_{k,\text{eff}}^H \mathbf{h}_{c,k}^r, \end{aligned} \quad (47)$$

where  $\mathbf{h}_{c,k}^r = \left[ \mathbf{w}_{c,k}^{r,T} \left( \mathbf{w}_{c,k}^{r,T} \otimes \mathbf{v}^{r,H} \right) \right]^T$ .

Based on (41), (46), and (47), we can compactly rewrite  $|\mathbf{v}^{r,H} \mathbf{F}_k \mathbf{w}_{c,k}^r + \mathbf{h}_{d,k}^H \mathbf{w}_{c,k}^r|^2$  in (41) as

$$\begin{aligned} & \left| \mathbf{v}^{r,H} \mathbf{F}_k \mathbf{w}_{c,k}^r + \mathbf{h}_{d,k}^H \mathbf{w}_{c,k}^r \right|^2 = \Delta \mathbf{h}_{k,\text{eff}}^H \mathbf{H}_{c,k}^r \Delta \mathbf{h}_{k,\text{eff}} + \\ & 2\text{Re}\left\{ \left( \hat{\mathbf{h}}_k^{r,H} \mathbf{w}_{c,k}^r \right)^H \Delta \mathbf{h}_{k,\text{eff}}^H \mathbf{h}_{c,k}^r \right\} + \left| \hat{\mathbf{h}}_k^{r,H} \mathbf{w}_{c,k}^r \right|^2. \end{aligned} \quad (48)$$

In addition, we can expand  $\left( \mathbf{v}^H \mathbf{F}_k \mathbf{w}_{c,k} + \mathbf{h}_{d,k}^H \mathbf{w}_{c,k} \right)^H \times \left( \mathbf{v}^{r,H} \mathbf{F}_k \mathbf{w}_{c,k}^r + \mathbf{h}_{d,k}^H \mathbf{w}_{c,k}^r \right)$  in (40) as

$$\begin{aligned} & \left( \mathbf{v}^H \mathbf{F}_k \mathbf{w}_{c,k} + \mathbf{h}_{d,k}^H \mathbf{w}_{c,k} \right)^H \left( \mathbf{v}^{r,H} \mathbf{F}_k \mathbf{w}_{c,k}^r + \mathbf{h}_{d,k}^H \mathbf{w}_{c,k}^r \right) = \\ & \mathbf{w}_{c,k}^H \hat{\mathbf{h}}_k \hat{\mathbf{h}}_k^{r,H} \mathbf{w}_{c,k}^r + \mathbf{w}_{c,k}^H \hat{\mathbf{h}}_k \mathbf{v}^{r,H} \Delta \mathbf{F}_k \mathbf{w}_{c,k}^r + \mathbf{w}_{c,k}^H \hat{\mathbf{h}}_k \Delta \mathbf{h}_{d,k}^H \mathbf{w}_{c,k}^r \\ & + \mathbf{w}_{c,k}^H \Delta \mathbf{F}_k^H \mathbf{v} \hat{\mathbf{h}}_k^{r,H} \mathbf{w}_{c,k}^r + \mathbf{w}_{c,k}^H \Delta \mathbf{F}_k^H \mathbf{v} \mathbf{v}^{r,H} \Delta \mathbf{F}_k \mathbf{w}_{c,k}^r + \\ & \mathbf{w}_{c,k}^H \Delta \mathbf{F}_k^H \mathbf{v} \Delta \mathbf{h}_{d,k}^H \mathbf{w}_{c,k}^r + \mathbf{w}_{c,k}^H \Delta \mathbf{h}_{d,k} \hat{\mathbf{h}}_k^{r,H} \mathbf{w}_{c,k}^r + \\ & \mathbf{w}_{c,k}^H \Delta \mathbf{h}_{d,k} \mathbf{v}^{r,H} \Delta \mathbf{F}_k \mathbf{w}_{c,k}^r + \mathbf{w}_{c,k}^H \Delta \mathbf{h}_{d,k} \Delta \mathbf{h}_{d,k}^H \mathbf{w}_{c,k}^r, \end{aligned} \quad (49)$$

where  $\hat{\mathbf{h}}_k^H = \mathbf{v}^H \hat{\mathbf{F}}_k + \hat{\mathbf{h}}_{d,k}^H$ . Similarly, we can transform terms in (49) as

$$\mathbf{w}_{c,k}^H \hat{\mathbf{h}}_k \mathbf{v}^{r,H} \Delta \mathbf{F}_k \mathbf{w}_{c,k}^r = \text{vec}^H(\Delta \mathbf{F}_k^*) \left( \mathbf{w}_{c,k}^{r,T} \otimes \mathbf{v}^{r,H} \right)^T \mathbf{w}_{c,k}^H \hat{\mathbf{h}}_k, \quad (50)$$

$$\mathbf{w}_{c,k}^H \Delta \mathbf{F}_k^H \mathbf{v} \hat{\mathbf{h}}_k^{r,H} \mathbf{w}_{c,k}^r = \hat{\mathbf{h}}_k^{r,H} \mathbf{w}_{c,k}^r \left( \mathbf{w}_{c,k}^H \otimes \mathbf{v}^T \right) \text{vec}(\Delta \mathbf{F}_k^*), \quad (51)$$

$$\begin{aligned} & \mathbf{w}_{c,k}^H \Delta \mathbf{F}_k^H \mathbf{v} \mathbf{v}^{r,H} \Delta \mathbf{F}_k \mathbf{w}_{c,k}^r = \\ & \text{vec}^H(\Delta \mathbf{F}_k^*) \left( \left( \mathbf{w}_{c,k}^r \mathbf{w}_{c,k}^H \right)^T \otimes (\mathbf{v} \mathbf{v}^{r,H}) \right)^T \text{vec}(\Delta \mathbf{F}_k^*), \end{aligned} \quad (52)$$

$$\begin{aligned} & \mathbf{w}_{c,k}^H \Delta \mathbf{F}_k^H \mathbf{v} \Delta \mathbf{h}_{d,k}^H \mathbf{w}_{c,k}^r = \\ & \Delta \mathbf{h}_{d,k}^H \left( \left( \mathbf{w}_{c,k}^r \mathbf{w}_{c,k}^H \right)^T \otimes \mathbf{v} \right)^T \text{vec}(\Delta \mathbf{F}_k^*). \end{aligned} \quad (53)$$

Thus,  $\left( \mathbf{v}^H \mathbf{F}_k \mathbf{w}_{c,k} + \mathbf{h}_{d,k}^H \mathbf{w}_{c,k} \right)^H \left( \mathbf{v}^{r,H} \mathbf{F}_k \mathbf{w}_{c,k}^r + \mathbf{h}_{d,k}^H \mathbf{w}_{c,k}^r \right)$  can be written in a more compact form given by

$$\begin{aligned} & \left( \mathbf{v}^H \mathbf{F}_k \mathbf{w}_{c,k} + \mathbf{h}_{d,k}^H \mathbf{w}_{c,k} \right)^H \left( \mathbf{v}^{r,H} \mathbf{F}_k \mathbf{w}_{c,k}^r + \mathbf{h}_{d,k}^H \mathbf{w}_{c,k}^r \right) = \\ & \Delta \mathbf{h}_{k,\text{eff}}^H \mathbf{H}_{c,k} \Delta \mathbf{h}_{k,\text{eff}} + \Delta \mathbf{h}_{k,\text{eff}}^H \mathbf{h}_{c,k}^r \mathbf{w}_{c,k}^H \hat{\mathbf{h}}_k + \\ & \hat{\mathbf{h}}_k^{r,H} \mathbf{w}_{c,k}^r \mathbf{h}_{c,k}^H \Delta \mathbf{h}_{k,\text{eff}} + \mathbf{w}_{c,k}^H \hat{\mathbf{h}}_k \hat{\mathbf{h}}_k^{r,H} \mathbf{w}_{c,k}^r, \end{aligned} \quad (54)$$

where  $\mathbf{h}_{c,k} = \left[ \mathbf{w}_{c,k}^T \left( \mathbf{w}_{c,k}^T \otimes \mathbf{v}^H \right) \right]^T$  and  $\mathbf{H}_{c,k} = \begin{bmatrix} \mathbf{w}_{c,k}^r \mathbf{w}_{c,k}^H & \left( \mathbf{w}_{c,k}^r \mathbf{w}_{c,k}^H \right) \otimes \mathbf{v}^T \\ \left( \mathbf{w}_{c,k}^r \mathbf{w}_{c,k}^H \right) \otimes \mathbf{v}^{r,*} & \left( \mathbf{w}_{c,k}^r \mathbf{w}_{c,k}^H \right) \otimes (\mathbf{v}^{r,*} \mathbf{v}^T) \end{bmatrix}$ .

As a result, based on (40), (48), and (54), constraint (38) can be approximated as

$$\begin{aligned} & \Delta \mathbf{h}_{k,\text{eff}}^H (\mathbf{H}_{c,k} + \mathbf{H}_{c,k}^H - \mathbf{H}_{c,k}^r) \Delta \mathbf{h}_{k,\text{eff}} + 2\text{Re}\left\{ \hat{\mathbf{h}}_k^H \Delta \mathbf{h}_{k,\text{eff}} \right\} \\ & + \bar{h}_{c,k} \geq \beta_{c,k} r_{k,\text{th}}, \Delta \mathbf{h}_{d,k} \in \mathcal{H}_{d,k}, \Delta \mathbf{F}_k \in \mathcal{F}_k, k \in \mathcal{K}, \end{aligned} \quad (55)$$

where  $\hat{\mathbf{h}}_k^H = \hat{\mathbf{h}}_k^H \mathbf{w}_{c,k} \mathbf{h}_{c,k}^H + \hat{\mathbf{h}}_k^{r,H} \mathbf{w}_{c,k}^r \mathbf{h}_{c,k}^H - \hat{\mathbf{h}}_k^{r,H} \mathbf{w}_{c,k}^r \mathbf{h}_{c,k}^H$  and  $\bar{h}_{c,k} = 2\text{Re}\left\{ \mathbf{w}_{c,k}^H \hat{\mathbf{h}}_k \hat{\mathbf{h}}_k^{r,H} \mathbf{w}_{c,k}^r \right\} - \left| \hat{\mathbf{h}}_k^{r,H} \mathbf{w}_{c,k}^r \right|^2$ . We note that (55) still involves an infinite number of inequality constraints.

To circumvent this difficulty, we convert the infinite number of constraints in (55) into an equivalent form with only a finite number of LMIs by applying the following lemma.

**Lemma 1:** (General  $\mathcal{S}$ -Procedure [42]) Let  $f_i(\mathbf{z}) = \mathbf{z}^H \mathbf{A}_i \mathbf{z} + 2\text{Re}\{\mathbf{b}_i^H \mathbf{z}\} + c_i, i \in \{0, 1, \dots, I\}$ , where  $\mathbf{z} \in \mathbb{C}^{N \times 1}$  and  $\mathbf{A}_i = \mathbf{A}_i^H \in \mathbb{C}^{N \times N}$ . The condition  $\{f_i(\mathbf{z}) \geq 0\}_{i=1}^I \Rightarrow f_0(\mathbf{z}) \geq 0$  holds if and only if there exist  $\lambda_i \geq 0, i \in \{1, \dots, I\}$  such that

$$\begin{bmatrix} \mathbf{A}_0 & \mathbf{b}_0 \\ \mathbf{b}_0^H & c_0 \end{bmatrix} - \sum_{i=1}^I \lambda_i \begin{bmatrix} \mathbf{A}_i & \mathbf{b}_i \\ \mathbf{b}_i^H & c_i \end{bmatrix} \succeq \mathbf{0}_{N+1}. \quad (56)$$

Before applying Lemma 1, we first re-express uncertainties  $\Delta \mathbf{h}_{d,k} \in \mathcal{H}_{d,k}$  and  $\Delta \mathbf{F}_k \in \mathcal{F}_k$  as

$$\Delta \mathbf{h}_{d,k} \in \mathcal{H}_{d,k} \Rightarrow \Delta \mathbf{h}_{k,\text{eff}}^H \begin{bmatrix} \mathbf{I}_N & \mathbf{0}_{N \times MN} \\ \mathbf{0}_{MN \times N} & \mathbf{0}_{MN} \end{bmatrix} \Delta \mathbf{h}_{k,\text{eff}} \leq \varepsilon_{d,k}^2, k \in \mathcal{K}, \quad (57)$$

$$\Delta \mathbf{F}_k \in \mathcal{F}_k \Rightarrow \Delta \mathbf{h}_{k,\text{eff}}^H \begin{bmatrix} \mathbf{0}_N & \mathbf{0}_{N \times MN} \\ \mathbf{0}_{MN \times N} & \mathbf{I}_{MN} \end{bmatrix} \Delta \mathbf{h}_{k,\text{eff}} \leq \varepsilon_k^2, k \in \mathcal{K}. \quad (58)$$

Then, based on Lemma 1, (55) can be transformed as

$$\begin{bmatrix} \mathbf{H}_{c,k} + \mathbf{H}_{c,k}^H - \mathbf{H}_{c,k}^r + \begin{bmatrix} \lambda_{1,k} \mathbf{I}_N & \mathbf{0}_{N \times MN} \\ \mathbf{0}_{MN \times N} & \lambda_{2,k} \mathbf{I}_{MN} \end{bmatrix} & \hat{\mathbf{h}}_{c,k} \\ & \hat{\mathbf{h}}_{c,k}^H \\ & c_k \end{bmatrix} \succeq \mathbf{0}_{N+MN+1}, k \in \mathcal{K}, \quad (59)$$

where  $c_k = \bar{h}_{c,k} - \beta_{c,k} r_{e,k,\text{th}} - \lambda_{1,k} \varepsilon_{d,k}^2 - \lambda_{2,k} \varepsilon_k^2, \lambda_{1,k} \geq 0$  and  $\lambda_{1,k} \geq 0$  represents the auxiliary variables corresponding to (57) and (58), respectively. It can be observed that (59) involves a finite number of LMIs, which thus can be handled using convex optimization techniques.

To tackle constraint (39), we first equivalently transform it into LMIs based on the Schur's complement given by

$$\begin{bmatrix} \beta_{c,k} - \sigma_k^2 & \mathbf{h}_k^H \mathbf{W}_{-k} \\ \mathbf{W}_{-k}^H \mathbf{h}_k & \mathbf{I}_{K-1+N} \end{bmatrix} \succeq \mathbf{0}_{K+N}, \Delta \mathbf{h}_{d,k} \in \mathcal{H}_{d,k}, \Delta \mathbf{F}_k \in \mathcal{F}_k, k \in \mathcal{K}, \quad (60)$$

where  $\mathbf{W}_{-k} = [\mathbf{w}_{c,1}, \dots, \mathbf{w}_{c,k-1}, \mathbf{w}_{c,k+1}, \dots, \mathbf{w}_{c,K}, \mathbf{w}_{r,1}, \dots, \mathbf{w}_{r,N}]$ . Substituting  $\mathbf{F}_k = \hat{\mathbf{F}}_k + \Delta \mathbf{F}_k$  and  $\mathbf{h}_{d,k} = \hat{\mathbf{h}}_{d,k} + \Delta \mathbf{h}_{d,k}$  into (60), this can then be expanded as

$$\begin{bmatrix} \beta_{c,k} - \sigma_k^2 & (\mathbf{v}^H \hat{\mathbf{F}}_k + \hat{\mathbf{h}}_{d,k}^H) \mathbf{W}_{-k} \\ \mathbf{W}_{-k}^H (\hat{\mathbf{F}}_k^H \mathbf{v} + \hat{\mathbf{h}}_{d,k}) & \mathbf{I}_{K-1+N} \end{bmatrix} + \begin{bmatrix} \mathbf{0}_{1 \times N} \\ \mathbf{W}_{-k}^H \end{bmatrix} \times \Delta \mathbf{h}_{d,k} \begin{bmatrix} 1 & \mathbf{0}_{1 \times (K-1+N)} \end{bmatrix} + \begin{bmatrix} 1 \\ \mathbf{0}_{(K-1+N) \times 1} \end{bmatrix} \Delta \mathbf{h}_{d,k}^H \times \begin{bmatrix} \mathbf{0}_{N \times 1} & \mathbf{W}_{-k} \end{bmatrix} + \begin{bmatrix} \mathbf{0}_{1 \times N} \\ \mathbf{W}_{-k}^H \end{bmatrix} \Delta \mathbf{F}_k^H \begin{bmatrix} \mathbf{v} & \mathbf{0}_{M \times (K-1+N)} \end{bmatrix} + \begin{bmatrix} \mathbf{v}^H \\ \mathbf{0}_{(K-1+N) \times M} \end{bmatrix} \Delta \mathbf{F}_k \begin{bmatrix} \mathbf{0}_{N \times 1} & \mathbf{W}_{-k} \end{bmatrix} \succeq \mathbf{0}_{K+N}, \Delta \mathbf{h}_{d,k} \in \mathcal{H}_{d,k}, \Delta \mathbf{F}_k \in \mathcal{F}_k, k \in \mathcal{K}. \quad (61)$$

To address the infinite number of LMIs in (61), we transform (61) into an equivalent form with only a finite number of LMIs by applying the following lemma:

**Lemma 2:** (General sign-definiteness [43]) Let  $\mathbf{Q} \succeq \sum_{i=1}^I (\mathbf{A}_i^H \mathbf{X}_i \mathbf{B}_i + \mathbf{B}_i^H \mathbf{X}_i^H \mathbf{A}_i)$  and  $\|\mathbf{X}_i\|_F \leq \varepsilon_i$ , where  $\mathbf{Q} = \mathbf{Q}^H$ . The condition  $\{\|\mathbf{X}_i\|_F \leq \varepsilon_i\}_{i=1}^I \Rightarrow \mathbf{Q} \succeq$

$\sum_{i=1}^I (\mathbf{A}_i^H \mathbf{X}_i \mathbf{B}_i + \mathbf{B}_i^H \mathbf{X}_i^H \mathbf{A}_i)$  holds if and only if there exist  $\lambda_i \geq 0, i \in \{1, \dots, I\}$  such that

$$\begin{bmatrix} \mathbf{Q} - \sum_{i=1}^I \bar{\lambda}_i \mathbf{B}_i^H \mathbf{B}_i & -\varepsilon_1 \mathbf{A}_1^H & \cdots & -\varepsilon_I \mathbf{A}_I^H \\ -\varepsilon_1 \mathbf{A}_1 & \bar{\lambda}_1 \mathbf{I} & \cdots & \mathbf{0} \\ \vdots & \vdots & \ddots & \vdots \\ -\varepsilon_I \mathbf{A}_I & \mathbf{0} & \cdots & \bar{\lambda}_I \mathbf{I} \end{bmatrix} \succeq \mathbf{0}. \quad (62)$$

Based on Lemma 2, (61) can be written as (63) (at the top of the next page), where  $\bar{\lambda}_{1,k} \geq 0$  and  $\bar{\lambda}_{2,k} \geq 0$  denote the corresponding auxiliary variables. To handle the uncertainty  $\Delta \mathbf{F}_r \in \mathcal{F}_r$  in constraint (12c), we introduce auxiliary variables  $\{\beta_{r,k} \geq 0\}$  satisfying  $\beta_{r,k} = \sum_{i \neq k}^K |\mathbf{g}^H \mathbf{w}_{c,i}|^2 + \sum_{n=1}^N |\mathbf{g}^H \mathbf{w}_{r,n}|^2 + \sigma_i^2, k \in \mathcal{K}$ , and constraint (12c) can be then equivalently transformed as

$$|\mathbf{g}^H \mathbf{w}_{c,k}|^2 \leq \beta_{r,k} r_{e,k,\text{th}}, \theta_h \in \Phi_h, \varphi_v \in \Phi_v, \Delta \mathbf{F}_r \in \mathcal{F}_r, k \in \mathcal{K}, \quad (64)$$

$$\sum_{i \neq k}^K |\mathbf{g}^H \mathbf{w}_{c,i}|^2 + \sum_{n=1}^N |\mathbf{g}^H \mathbf{w}_{r,n}|^2 + \sigma_i^2 \geq \beta_{r,k}, \theta_h \in \Phi_h, \varphi_v \in \Phi_v, \Delta \mathbf{F}_r \in \mathcal{F}_r, k \in \mathcal{K}. \quad (65)$$

Similar to the constraint (39), we first transform the inequalities in (64) into LMIs by applying Schur's complement, which yields

$$\begin{bmatrix} \beta_{r,k} r_{e,k,\text{th}} & \mathbf{g}^H \mathbf{w}_{c,k} \\ \mathbf{w}_{c,k}^H \mathbf{g} & 1 \end{bmatrix} \succeq \mathbf{0}_2, \theta_h \in \Phi_h, \varphi_v \in \Phi_v, \Delta \mathbf{F}_r \in \mathcal{F}_r, k \in \mathcal{K}. \quad (66)$$

Recalling that  $\mathbf{g}^H = \mathbf{v}^H \mathbf{F}_r$  and substituting  $\mathbf{F}_r = \hat{\mathbf{F}}_r + \Delta \mathbf{F}_r$  into (66), the following inequalities are obtained

$$\begin{bmatrix} \beta_{r,k} r_{e,k,\text{th}} & \mathbf{v}^H \hat{\mathbf{F}}_r \mathbf{w}_{c,k} \\ \mathbf{w}_{c,k}^H \hat{\mathbf{F}}_r^H \mathbf{v} & 1 \end{bmatrix} + \begin{bmatrix} \mathbf{v}^H \\ \mathbf{0}_{1 \times M} \end{bmatrix} \Delta \mathbf{F}_r \begin{bmatrix} \mathbf{0}_{N \times 1} & \mathbf{w}_{c,k} \end{bmatrix} + \begin{bmatrix} \mathbf{0}_{1 \times N} \\ \mathbf{w}_{c,k}^H \end{bmatrix} \Delta \mathbf{F}_r^H \begin{bmatrix} \mathbf{v} & \mathbf{0}_{M \times 1} \end{bmatrix} \succeq \mathbf{0}_2, \theta_h \in \Phi_h, \varphi_v \in \Phi_v, \Delta \mathbf{F}_r \in \mathcal{F}_r. \quad (67)$$

Based on Lemma 2, constraint (67) involving an infinite number of inequalities can be recast as a finite number of LMIs given by

$$\begin{bmatrix} \beta_{r,k} r_{e,k,\text{th}} - \bar{\lambda}_k M & \mathbf{v}^H \hat{\mathbf{F}}_r \mathbf{w}_{c,k} & \mathbf{0}_{1 \times N} \\ \mathbf{w}_{c,k}^H \hat{\mathbf{F}}_r^H \mathbf{v} & 1 & -\varepsilon_r \mathbf{w}_{c,k}^H \\ \mathbf{0}_{N \times 1} & -\varepsilon_r \mathbf{w}_{c,k} & \bar{\lambda}_k \mathbf{I}_N \end{bmatrix} \succeq \mathbf{0}_{N+2}, \theta_h \in \Phi_h, \varphi_v \in \Phi_v, k \in \mathcal{K}, \quad (68)$$

where  $\bar{\lambda}_k \geq 0$  represents the corresponding auxiliary variables.

Although constraint (65) is not convex w.r.t  $\mathbf{v}$ , the left-hand side of (65) is a quadratic function of  $\mathbf{v}$ . Thus, we can obtain the following lower bound for  $|\mathbf{g}^H \mathbf{w}_{p,i}|^2, p \in \{c, r\}, i \in \mathcal{K} \cup \mathcal{N}$  at any point  $\mathbf{v}^r$

$$|\mathbf{g}^H \mathbf{w}_{p,i}|^2 \geq -|\mathbf{v}^{r,H} \mathbf{F}_r \mathbf{w}_{p,i}^r|^2 + 2\text{Re}\left\{(\mathbf{v}^{r,H} \mathbf{F}_r \mathbf{w}_{p,i}^r)^H (\mathbf{v}^{r,H} \mathbf{F}_r \mathbf{w}_{p,i}^r)\right\}. \quad (69)$$

Substituting  $\mathbf{F}_r = \hat{\mathbf{F}}_r + \Delta \mathbf{F}_r$  into  $|\mathbf{v}^{r,H} \mathbf{F}_r \mathbf{w}_{p,i}^r|^2$ , we have

$$\begin{aligned} & \left| \mathbf{v}^{r,H} \hat{\mathbf{F}}_r \mathbf{w}_{p,i}^r + \mathbf{v}^{r,H} \Delta \mathbf{F}_r \mathbf{w}_{p,i}^r \right|^2 = \left| \mathbf{v}^{r,H} \hat{\mathbf{F}}_r \mathbf{w}_{p,i}^r \right|^2 + \\ & \text{vec}^H(\Delta \mathbf{F}_r^*) \left( \left( \mathbf{w}_{p,i}^r \mathbf{w}_{p,i}^{r,H} \right)^T \otimes \left( \mathbf{v}^r \mathbf{v}^{r,H} \right) \right)^T \text{vec}(\Delta \mathbf{F}_r^*) + \\ & 2\text{Re}\left\{ \mathbf{v}^{r,H} \hat{\mathbf{F}}_r \mathbf{w}_{p,i}^r \left( \mathbf{w}_{p,i}^{r,H} \otimes \mathbf{v}^{r,T} \right) \text{vec}(\Delta \mathbf{F}_r^*) \right\}. \quad (70) \end{aligned}$$



$$\begin{bmatrix} \beta_{c,k} - \sigma_k^2 - \bar{\lambda}_{1,k} - \bar{\lambda}_{2,k}M & \left( \mathbf{v}^H \hat{\mathbf{F}}_k + \hat{\mathbf{h}}_{d,k}^H \right) \mathbf{W}_{-k} & \mathbf{0}_{1 \times N} & \mathbf{0}_{1 \times N} \\ \mathbf{W}_{-k}^H \left( \hat{\mathbf{F}}_k^H \mathbf{v} + \hat{\mathbf{h}}_{d,k} \right) & \mathbf{I}_{K-1+N} & -\varepsilon_{d,k} \mathbf{W}_{-k}^H & -\varepsilon_k \mathbf{W}_{-k}^H \\ \mathbf{0}_{N \times 1} & -\varepsilon_{d,k} \mathbf{W}_{-k} & \bar{\lambda}_{1,k} \mathbf{I}_N & \mathbf{0}_N \\ \mathbf{0}_{N \times 1} & -\varepsilon_k \mathbf{W}_{-k} & \mathbf{0}_N & \bar{\lambda}_{2,k} \mathbf{I}_N \end{bmatrix} \succ \mathbf{0}_{K+3N}, k \in \mathcal{K}, \quad (63)$$

In addition, substituting  $\mathbf{F}_r = \hat{\mathbf{F}}_r + \Delta \mathbf{F}_r$  into  $(\mathbf{v}^H \mathbf{F}_r \mathbf{w}_{p,i})^H (\mathbf{v}^{r,H} \mathbf{F}_r \mathbf{w}_{p,i}^r)$ , we have

$$\begin{aligned} (\mathbf{v}^H \mathbf{F}_r \mathbf{w}_{p,i})^H (\mathbf{v}^{r,H} \mathbf{F}_r \mathbf{w}_{p,i}^r) &= \mathbf{w}_{p,i}^H \hat{\mathbf{F}}_r^H \mathbf{v} \mathbf{v}^{r,H} \hat{\mathbf{F}}_r \mathbf{w}_{p,i}^r + \mathbf{w}_{p,i}^H \times \\ &\hat{\mathbf{F}}_r^H \mathbf{v} \text{vec}^H(\Delta \mathbf{F}_r^*) (\mathbf{w}_{p,i}^r \otimes \mathbf{v}^{r,*}) + \mathbf{v}^{r,H} \hat{\mathbf{F}}_r \mathbf{w}_{p,i}^r (\mathbf{w}_{p,i}^H \otimes \mathbf{v}^T) \times \\ &\text{vec}(\Delta \mathbf{F}_r^*) + \text{vec}^H(\Delta \mathbf{F}_r^*) ((\mathbf{w}_{p,i}^r \mathbf{w}_{p,i}^H) \otimes (\mathbf{v}^{r,*} \mathbf{v}^T)) \text{vec}(\Delta \mathbf{F}_r^*). \end{aligned} \quad (71)$$

Based on (69), (70), and (71), a lower bound for constraint (65) is given by

$$\begin{aligned} \text{vec}^H(\Delta \mathbf{F}_r^*) \mathbf{H}_{\text{temp}} \text{vec}(\Delta \mathbf{F}_r^*) + \left( \sum_{i \neq k}^K c_{c,i} + \sum_{n=1}^N c_{r,n} \right) + \sigma_i^2 + \\ 2\text{Re} \left\{ \left( \sum_{i \neq k}^K \hat{\mathbf{g}}_{c,i}^H + \sum_{n=1}^N \hat{\mathbf{g}}_{r,i}^H \right) \text{vec}(\Delta \mathbf{F}_r^*) \right\} \geq \beta_{r,k}, \theta_h \in \Phi_h, \\ \varphi_v \in \Phi_v, \Delta \mathbf{F}_r \in \mathcal{F}_r, k \in \mathcal{K}, \end{aligned} \quad (72)$$

where  $\mathbf{H}_{-k} = \sum_{i \neq k}^K (\bar{\mathbf{H}}_{c,i} + \bar{\mathbf{H}}_{c,i}^H - \bar{\mathbf{H}}_{c,i}^r) + \sum_{n=1}^N (\bar{\mathbf{H}}_{r,n} + \bar{\mathbf{H}}_{r,n}^H - \bar{\mathbf{H}}_{r,n}^r)$ ,  $\bar{\mathbf{H}}_{p,i} = (\mathbf{w}_{p,i}^r \mathbf{w}_{p,i}^H) \otimes (\mathbf{v}^{r,*} \mathbf{v}^T)$ ,  $\bar{\mathbf{H}}_{p,i}^r = (\mathbf{w}_{p,i}^r \mathbf{w}_{p,i}^{r,H}) \otimes (\mathbf{v}^r \mathbf{v}^{r,H})^T$ ,  $\hat{\mathbf{g}}_{p,i}^H = \mathbf{v}^H \hat{\mathbf{F}}_r \mathbf{w}_{p,i} (\mathbf{w}_{p,i}^{r,H} \otimes \mathbf{v}^{r,T}) + \mathbf{v}^{r,H} \hat{\mathbf{F}}_r \mathbf{w}_{p,i}^r (\mathbf{w}_{p,i}^H \otimes \mathbf{v}^T) - \mathbf{v}^{r,H} \hat{\mathbf{F}}_r \mathbf{w}_{p,i}^r (\mathbf{w}_{p,i}^{r,H} \otimes \mathbf{v}^{r,T})$ , and  $c_{p,i} = 2\text{Re} \left\{ \mathbf{w}_{p,i}^H \hat{\mathbf{F}}_r^H \mathbf{v} \mathbf{v}^{r,H} \hat{\mathbf{F}}_r \mathbf{w}_{p,i}^r \right\} - \left| \mathbf{v}^{r,H} \hat{\mathbf{F}}_r \mathbf{w}_{p,i}^r \right|^2$ . Thus, based on Lemma 1, constraint (72) can be transformed to a finite number of LMIs given by

$$\begin{bmatrix} \mathbf{H}_{-k} + \lambda_{r,k} \mathbf{I}_{MN} & \left( \sum_{i \neq k}^K \hat{\mathbf{g}}_{c,i}^H + \sum_{n=1}^N \hat{\mathbf{g}}_{r,i}^H \right)^H \\ \sum_{i \neq k}^K \hat{\mathbf{g}}_{c,i}^H + \sum_{n=1}^N \hat{\mathbf{g}}_{r,i}^H & \left( \sum_{i \neq k}^K c_{c,i} + \sum_{n=1}^N c_{r,n} \right) + c_{0,k} \end{bmatrix} \succeq \mathbf{0}_{MN+1}, \theta_h \in \Phi_h, \varphi_v \in \Phi_v, k \in \mathcal{K}, \quad (73)$$

where  $c_{0,k} = \sigma_i^2 - \beta_{r,k} - \lambda_{r,k} \varepsilon_r^2$  and  $\lambda_{r,k} \geq 0$  denote the corresponding auxiliary variables.

As a result, problem (12) can be recast as

$$\max_{\{\mathbf{w}_{c,k}\}, \{\mathbf{w}_{r,n}\}, \{v_m\}, \{\beta_{c,k}\}, \bar{\lambda}, \{\bar{\lambda}_{1,k}, \bar{\lambda}_{2,k}, \lambda_{1,k}, \lambda_{2,k}, \lambda_{r,k}\}, \chi} \chi \quad (74a)$$

$$\text{s.t. } \mathbf{g}^H \left( \sum_{k=1}^K \mathbf{w}_{c,k} \mathbf{w}_{c,k}^H + \sum_{n=1}^N \mathbf{w}_{r,n} \mathbf{w}_{r,n}^H \right) \mathbf{g} \geq \chi, \theta_h \in \Phi_h, \\ \varphi_v \in \Phi_v, \Delta \mathbf{F}_r \in \mathcal{F}_r, \quad (74b)$$

$$(12d), (12e), (59), (63), (68), (73). \quad (74c)$$

Similarly, by applying Lemma 1, constraint (74b) can be recast as

$$\begin{bmatrix} \bar{\mathbf{H}}_{\text{temp}} + \tilde{\lambda}_r \mathbf{I}_{MN} & \left( \sum_{i=1}^K \hat{\mathbf{g}}_{c,i}^H + \sum_{n=1}^N \hat{\mathbf{g}}_{r,i}^H \right)^H \\ \sum_{i=1}^K \hat{\mathbf{g}}_{c,i}^H + \sum_{n=1}^N \hat{\mathbf{g}}_{r,i}^H & \left( \sum_{i \neq k}^K c_{c,i} + \sum_{n=1}^N c_{r,n} \right) - \chi - \tilde{\lambda}_r \varepsilon_r^2 \end{bmatrix} \succeq \mathbf{0}_{MN+1}, \theta_h \in \Phi_h, \varphi_v \in \Phi_v, \quad (75)$$

**Algorithm 2** The AO algorithm for solving problem (12).

- 1: **Initialize**  $v_m$  and  $\varepsilon$ .
- 2: **repeat**
- 3:     Update BS beamformers by solving problem (76).
- 4:     Update IRS phase shifts by solving problem (80).
- 5: **until** the fractional increase of the objective value is less than  $\varepsilon$ .

where  $\bar{\mathbf{H}}_{\text{temp}} = \sum_{i=1}^K (\bar{\mathbf{H}}_{c,i} + \bar{\mathbf{H}}_{c,i}^H - \bar{\mathbf{H}}_{c,i}^r) + \sum_{n=1}^N (\bar{\mathbf{H}}_{r,n} + \bar{\mathbf{H}}_{r,n}^H - \bar{\mathbf{H}}_{r,n}^r)$  and  $\lambda_r$  is the auxiliary variable. To solve problem (74), an AO algorithm is proposed to alternatively optimize transformers and IRS phase shifts until convergence is reached. Below, we elaborate on how to solve these two subproblems.

1) *Optimizing BS beamformers with fixed IRS phase shifts:*

This subproblem is given by

$$\max_{\{\mathbf{w}_{c,k}, \mathbf{w}_{r,n}, \beta_{c,k}, \bar{\lambda}_k, \bar{\lambda}_{1,k}, \bar{\lambda}_{2,k}, \lambda_{1,k}, \lambda_{2,k}, \lambda_{r,k}\}, \chi} \chi \quad (76a)$$

$$\text{s.t. (12d), (59), (63), (68), (73), (75).} \quad (76b)$$

It can be readily verified that problem (76) is a semi-definite program (SDP), which can be efficiently tackled by standard convex optimization solvers.

2) *Optimizing IRS phase shifts with fixed BS beamformers:*

This subproblem is written as

$$\max_{\{v_m, \beta_{c,k}, \bar{\lambda}_k, \bar{\lambda}_{1,k}, \bar{\lambda}_{2,k}, \lambda_{1,k}, \lambda_{2,k}, \lambda_{r,k}\}, \chi} \chi \quad (77a)$$

$$\text{s.t. (12e), (59), (63), (68), (73), (75).} \quad (77b)$$

It can be observed that all constraints are convex except (12e) due to the unit-modulus constraint, which is in general difficult to tackle. Fortunately, by applying the square penalty approach [44], problem (77) is equivalent to

$$\max_{\{v_m, \beta_{c,k}, \bar{\lambda}_k, \bar{\lambda}_{1,k}, \bar{\lambda}_{2,k}, \lambda_{1,k}, \lambda_{2,k}, \lambda_{r,k}\}, \chi} \chi + \bar{\rho} \|\mathbf{v}\|^2 \quad (78a)$$

$$\text{s.t. } |v_m| \leq 1, m \in \mathcal{M}, \quad (78b)$$

$$(59), (63), (68), (73), (75), \quad (78c)$$

where  $\bar{\rho}$  represents a sufficiently large positive penalty parameter used to make constraint (78b) met with equality at the optimal solution. Note that this equivalence does not require gradually adjusting  $\bar{\rho}$  as a large  $\bar{\rho}$  suffices. The rigorous proof can be found in [44, Theorem 1] for details. To tackle the non-convex objective function in (78), a lower bound for  $\|\mathbf{v}\|^2$  is obtained by applying the SCA. Specifically, for any given  $\mathbf{v}^r$ , we have

$$\|\mathbf{v}\|^2 \geq -\|\mathbf{v}^r\|^2 + 2\text{Re} \{ \mathbf{v}^H \mathbf{v}^r \}, \quad (79)$$

which is linear w.r.t.  $\mathbf{v}$ .

As a result, based on (79) and dropping irrelevant terms, problem (78) can be approximated as

$$\max_{\{v_m, \beta_{c,k}, \bar{\lambda}_k, \bar{\lambda}_{1,k}, \bar{\lambda}_{2,k}, \lambda_{1,k}, \lambda_{2,k}, \lambda_{r,k}\}, \chi} \chi + 2\bar{\rho} \text{Re} \{ \mathbf{v}^H \mathbf{v}^r \} \quad (80a)$$

$$\text{s.t. (59), (63), (68), (73), (75), (78b),} \quad (80b)$$

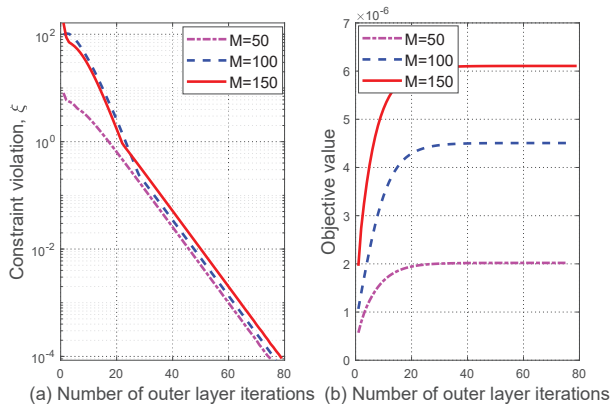


Fig. 2. Convergence behaviour of Algorithm 1 under  $P_{\max} = 40$  dBm,  $r_{c,\text{th}} = 10$  dB, and  $r_{e,\text{th}} = 0$  dB.

which is convex and can be solved by convex optimization solvers.

Finally, we alternately optimize the above two subproblems, and the details are summarized in Algorithm 2. Since problems (76) and (80) are SDPs, the complexity of Algorithm 2 is given by  $\mathcal{O}\left(L\left(K\left((N+MN+1)^{6.5} + (K+3N)^{6.5}\right) + \bar{K}(N+2)^{6.5} + (\bar{K}+1)(MN+1)^{6.5}\right)\right)$ , where  $L$  stands for the number of iterations required for reaching convergence and  $\bar{K}$  denotes the number of LMIs in (68) and (73).

## V. NUMERICAL RESULTS

In this section, we provide numerical results to validate the secure transmission performance in the IRS-aided ISAC system. A three dimensional coordinate setup measured in meters (m) is considered, where the BS is located at (0, 0, 2.5) m and the users are uniformly and randomly distributed in a circle of a radius 2 m centered at (20, 5, 0) m, while the IRS is deployed at (20, 0, 2.5) m. The distance-dependent path loss model is given by  $L(\hat{d}) = c_0(\hat{d}/d_0)^{-\hat{\alpha}}$ , where  $c_0 = -30$  dB is the path loss at the reference distance  $d_0 = 1$  m,  $\hat{d}$  is the link distance, and  $\hat{\alpha}$  is the path loss exponent. The target is located at azimuth direction  $\theta = -30^\circ$  and elevation direction  $\varphi = 40^\circ$ . We assume that the distance between the IRS and the target is 10 m with a path loss exponent of 2, and assume that the BS-IRS link and the IRS-user link follow Rician fading with a Rician factor of 3 dB and a path loss exponent of 2.2, while the BS-user link follows Rayleigh fading with a path loss exponent of 3.6. The minimum communication SINR and the maximum tolerable intercepting SINR are assumed to be the same for all users, i.e.,  $r_{c,\text{th}} = r_{k,\text{th}}, r_{e,\text{th}} = r_{e,k,\text{th}}, k \in \mathcal{K}$ . Unless otherwise specified, we set  $N = 4$ ,  $K = 3$ ,  $\theta = -30^\circ$ ,  $\varphi = 40^\circ$ ,  $\sigma_t^2 = \sigma_k^2 = -90$  dBm,  $\forall k$ ,  $\rho = 0.1$ ,  $c = 0.85$ ,  $\varepsilon_{\text{in}} = 10^{-2}$ , and  $\varepsilon = \varepsilon_{\text{out}} = 10^{-4}$ .

### A. Perfect CSI and Known Target Location

In this subsection, we consider the ideal case where the CSI and the target location are known at the BS, and the penalty-based algorithm, i.e., Algorithm 1, is employed.

1) *Convergence Behavior of Algorithm 1:* We first study the convergence behavior of Algorithm 1 for different numbers of IRS reflecting elements, namely  $M = 50$ ,  $M = 100$ , and  $M = 150$ , as shown in Fig. 2. It is observed from Fig. 2(a) that the constraint violation parameter  $\xi$  converges very rapidly

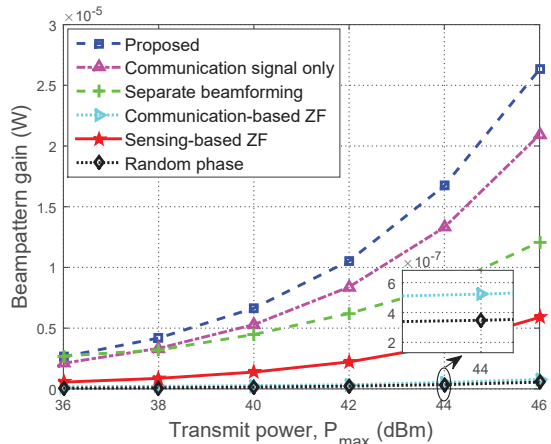


Fig. 3. Beampattern gain versus  $P_{\max}$  under  $M = 100$ ,  $r_{c,\text{th}} = 10$  dB, and  $r_{e,\text{th}} = 0$  dB.

to a predefined accuracy  $10^{-4}$  after about 75-80 iterations for all values of  $M$ . Note that the predefined accuracy value of  $10^{-4}$  is sufficiently small for ensuring that constraint (13d) is essentially met with equality at the optimal solution, since we normalize the channel coefficients by the noise power so that the auxiliary variables are inherently large to guarantee sufficient numerical accuracy. To see it more clearly, we can observe from Fig. 2(b) that the objective value of problem (14) converges quickly for different  $M$ , which demonstrates the efficiency of Algorithm 1.

To show the superiority of the proposed approach, we consider the following approaches for comparison.

- **Proposed approach:** This is our proposed approach described in Algorithm 1 in Section III.
- **Communication signal only:** Similar to the proposed approach, but without dedicated radar waveforms.
- **Separate beamforming:** This approach optimizes the transmit beamformers and IRS phase shifts separately. The algorithm first obtains the IRS phase-shift matrix by maximizing the norm of the IRS's cascaded channel towards the desired sensing target, i.e.,  $\max_{\Theta} \|\mathbf{g}_r^H \Theta \mathbf{G}\|$ . Then, with the obtained  $\Theta$ , the transmit beamformers are obtained by solving problem (8).
- **Communication-based zero-forcing (ZF):** The IRS phase-shift matrix is obtained in the same way as the separate beamforming approach, while the communication beamformers,  $\mathbf{w}_{c,k}, k \in \mathcal{K}$ , are forced to lie in the null space of the target's channel, i.e.,  $\mathbf{g}^H \mathbf{w}_{c,k} = 0, k \in \mathcal{K}$ . The communication covariance matrices are given by  $\mathbf{W}_{c,k} = (\mathbf{I}_N - \mathbf{g}\mathbf{g}^H / \|\mathbf{g}\|^2) \hat{\mathbf{W}}_{c,k} (\mathbf{I}_N - \mathbf{g}\mathbf{g}^H / \|\mathbf{g}\|^2)^H$ , where  $\text{rank}(\hat{\mathbf{W}}_{c,k}) = 1, \hat{\mathbf{W}}_{c,k} \succeq \mathbf{0}_N$ . Then,  $\hat{\mathbf{W}}_{c,k}$  and the radar covariance matrices are jointly optimized by using the AO algorithm.
- **Sensing-based ZF:** Similar to the communication-based ZF approach, the radar beamformers, i.e.,  $\mathbf{w}_{r,n}, n \in \mathcal{N}$ , are forced to lie in the null space of the users' channels i.e.,  $\mathbf{h}_k^H \mathbf{w}_{r,n} = 0, k \in \mathcal{K}, n \in \mathcal{N}$ . The radar beamformers are designed as  $\mathbf{W}_r = \mathbf{V} \hat{\mathbf{W}}_r$ , where  $\mathbf{V}$  represents the last  $N - K$  right singular vectors of  $\mathbf{H} = [\mathbf{h}_1, \dots, \mathbf{h}_K]^H$ . Then, the communication beamformers and  $\hat{\mathbf{W}}_r$  are jointly optimized by using the penalty-based algorithm.
- **Random phase:** The IRS phase shifts are generated randomly following a uniform distribution over  $[0, 2\pi)$ .

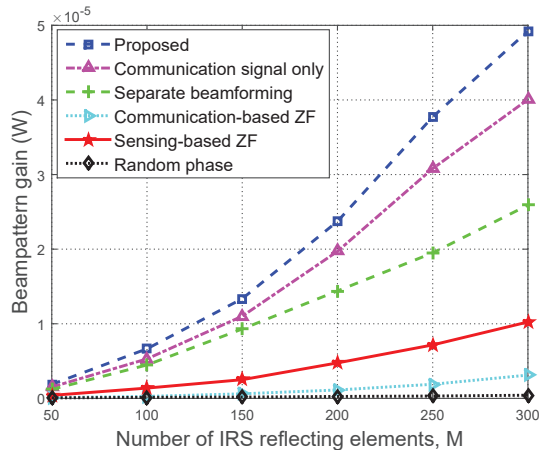


Fig. 4. Beampattern gain versus  $M$  under  $P_{\max} = 40$  dBm,  $r_{c,\text{th}} = 10$  dB, and  $r_{e,\text{th}} = 0$  dB.

2) *Beampattern Gain Versus Transmit Power*: In Fig. 3, we compare the beampattern gain of the above approaches versus  $P_{\max}$ . We see that the beampattern gain for all methods increases monotonically with  $P_{\max}$  since the co-channel interference is suppressed and increasing the available power improves the beampattern gain. In addition, we observe that the proposed approach outperforms the “Communication signal only” case, which indicates the benefit of dedicated radar signals. This can be explained as follows. The additional radar signals provide more DoFs for algorithm optimization, which improves the system performance, and to prevent the eavesdropping by the target, more power must be allocated to the radar signals and the beampattern gain is thus increased. Moreover, we observe that the beampattern gain obtained by the approaches without IRS phase shift optimization increases marginally as  $P_{\max}$  increases since the signals reflected by the IRS in this case are propagated in many random directions, thus results in a low received power level. Furthermore, compared to the “Separate beamforming”, “Communication-based ZF”, and “Sensing-based ZF” approaches, our proposed approach achieves significant beampattern gains, which illustrates the benefit of joint design of the transmit beamformers and IRS phase shifts.

3) *Beampattern Gain Versus Number of IRS Reflecting Elements*: In Fig. 4, we compare the beampattern gain for all approaches versus  $M$ . It is observed that the proposed approach outperforms the “Random phase” approach, and the system performance gap is more pronounced for a larger  $M$ . This is because installing more passive reflecting elements provides more DoFs for resource allocation, which is beneficial for achieving higher beamforming gain, thereby improving the beampattern gain when the IRS phase shifts are well adjusted. In addition, we again observe that our proposed approach outperforms the use of only communication signals, further amplifying the benefit of using dedicated radar signals. Moreover, the performance gap between our proposed approach and the “Separate beamforming”, “Communication-based ZF”, and “Sensing-based ZF” approaches is magnified as  $M$  increases, which again demonstrates the benefit of joint design of the transmit beamformers and IRS phase shifts.

4) *Beampattern Gain Versus Minimum SINR Required by Communication Users*: In Fig. 5, the achieved beampattern gain is plotted versus the communication users’ SINR requirement  $r_{c,\text{th}}$ . As expected, a more stringent QoS requirement for the users results in a lower beamforming gain to the target, since the

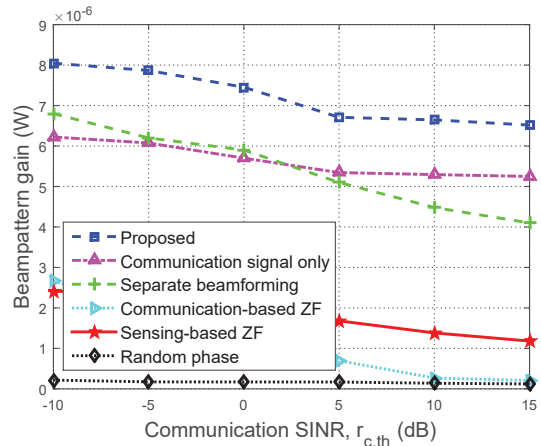


Fig. 5. Beampattern gain versus  $r_{c,\text{th}}$  under  $M = 100$ ,  $P_{\max} = 40$  dBm, and  $r_{e,\text{th}} = 0$  dB.

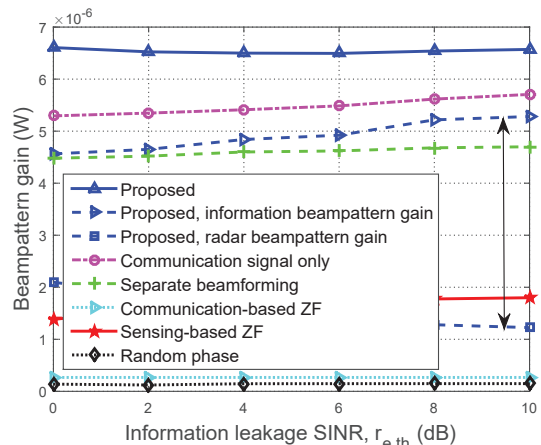


Fig. 6. Beampattern gain versus  $r_{e,\text{th}}$  under  $M = 100$ ,  $P_{\max} = 40$  dBm, and  $r_{c,\text{th}} = 10$  dB.

BS and IRS must focus more energy towards the communication users. In addition, we observe that the performance gap between our proposed approach and the “Separate beamforming” approach becomes smaller as  $r_{c,\text{th}}$  decreases. This is because in this case the SINR at the users can be easily satisfied, and thus extra radar and communication power can be used to improve the beampattern gain. Moreover, we observe that the performance of the “Communication-based ZF” approach degrades quickly as  $r_{c,\text{th}}$  increases. This is because communication signals are forced to lie in the null space of target’s channel, which indicates that no user information is leaked to the target and only the radar signals can be used to increase the beampattern gain. On the other hand, increasing the radar power potentially degrades the user SINR, which limits the improvement of beampattern gain.

5) *Beampattern Gain Versus Maximum Information Leakage SINR to Target*: We further study the beampattern gain versus the leakage constraint  $r_{e,\text{th}}$  in Fig. 6. Interestingly, we observe that the beampattern gain obtained by the proposed approach remains nearly unchanged with  $r_{e,\text{th}}$ . To unveil the reason behind this, the separate radar and communication power contributions to the beampattern gain versus  $r_{e,\text{th}}$  are studied, i.e.,  $\sum_{n=1}^N |\mathbf{w}_{r,n}^H \mathbf{g}|^2$  and  $\sum_{k=1}^K |\mathbf{w}_{c,k}^H \mathbf{g}|^2$ , which correspond to the “Proposed, radar beampattern gain” and the “Proposed, information beampattern gain” approaches, respectively. We

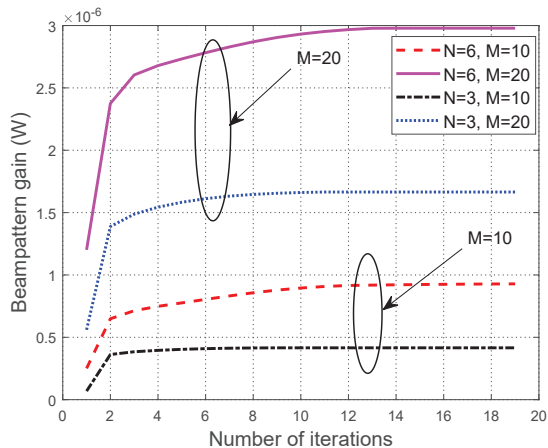


Fig. 7. Convergence behaviour of Algorithm 2 for different  $M$  and  $N$ .

see that as the requirement on signal leakage to the target is made less stringent (i.e.,  $r_{e,\text{th}}$  increases), less transmit power is allocated to radar signals to deteriorate the reception by the eavesdropping target, while more power is allocated to the information signals to improve the communication QoS. In the end, these two trends offset each other, and the sum of the two components results in a nearly constant beampattern gain. In addition, we observe that the performance gain obtained by the ‘‘Sensing-based ZF’’ approach increases marginally as  $r_{e,\text{th}}$  increases due to the limited DoFs available for design of the radar beamformers.

### B. Imperfect CSI and Uncertain Target Location

In this subsection, we consider the case with imperfect CSI and an unknown target location, and we propose Algorithm 2 to address the resulting problem. The azimuth and elevation target location ranges are set to  $\Phi_h = [-35^\circ, -25^\circ]$  and  $\Phi_v = [35^\circ, 45^\circ]$ , respectively. We define the relative amount of CSI errors as  $\hat{\epsilon}_r = \epsilon_r / \|\Delta \mathbf{F}_r\|_F$ ,  $\hat{\epsilon}_k = \epsilon_k / \|\Delta \mathbf{F}_k\|_F$ , and  $\hat{\epsilon}_{d,k} = \epsilon_{d,k} / \|\Delta \mathbf{h}_{d,k}\|$ ,  $\forall k$ , respectively. For ease of exposition, we assume that all channels have the same level of CSI errors and define  $\epsilon_{\text{error}} = \hat{\epsilon}_r = \hat{\epsilon}_k = \hat{\epsilon}_{d,k}$ ,  $\forall k$ .

1) *Convergence Behavior of Algorithm 2*: In Fig. 7, the convergence behaviour of Algorithm 2 for different  $M$  and  $N$  under  $\epsilon_{\text{error}} = 0.01$ ,  $P_{\text{max}} = 46$  dBm,  $K = 2$ ,  $r_{c,\text{th}} = 10$  dB, and  $r_{e,\text{th}} = 5$  dB is studied. It is observed that the obtained beampattern gain is monotonically increasing with the number of iterations and ultimately converges. Even for  $M = 20$  and  $N = 6$ , the proposed algorithm converges in about 20 iterations, which demonstrates the effectiveness of Algorithm 2.

2) *Beampattern Design*: In Fig. 8, we study the normalized beampattern obtained in the case with perfect CSI and the known target location and with the case of imperfect CSI and uncertain target location when  $M = 20$ ,  $N = 3$ ,  $\epsilon_{\text{error}} = 0.01$ ,  $P_{\text{max}} = 46$  dBm,  $K = 2$ ,  $r_{c,\text{th}} = 10$  dB, and  $r_{e,\text{th}} = 5$  dB. Both beampatterns are normalized by the maximum value of these two beampatterns. It is observed that both of the beampatterns obtained by our proposed algorithms correctly focus their mainlobe towards the directions  $\theta = -30^\circ$  and  $\varphi = 40^\circ$ . In addition, we observe that both beampatterns have sidelobe regions due to the imposed SINR constraints for the users as well as the information leakage to the eavesdropping target. Furthermore, we observe that the mainlobe in the imperfect CSI case is more flat and wide than that with perfect CSI case. This

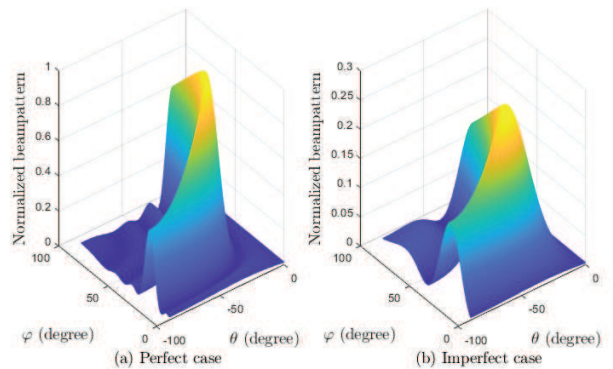


Fig. 8. Beampattern design for different system setups.

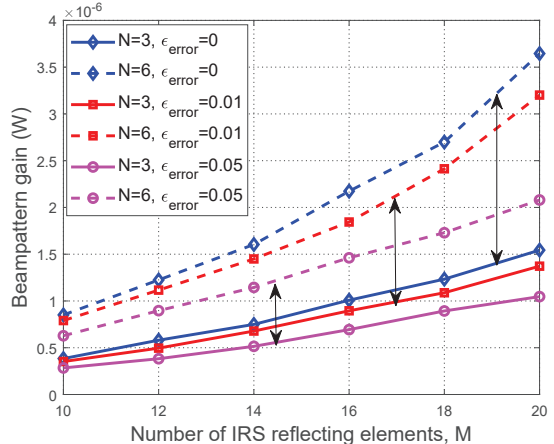


Fig. 9. Beampattern gain versus  $M$  for different  $N$  and  $\epsilon_{\text{error}}$ .

is expected since although the exact target location is unknown, its range of possible locations is known, so that the probing power should uniformly cover this area rather than focusing on a point in one direction. Moreover, we observe that the peak beampattern gain of the imperfect CSI case is lower than with in the perfect CSI case due to the reduced available information.

3) *Beampattern Gain Versus  $M$* : In Fig. 9, we study the beampattern gain versus  $M$  for different  $N$  and  $\epsilon_{\text{error}}$  under  $P_{\text{max}} = 46$  dBm,  $K = 2$ ,  $r_{e,\text{th}} = 5$  dB, and  $r_{c,\text{th}} = 10$  dB. A large  $\epsilon_{\text{error}}$  indicates that the channel estimation error is magnified and  $\epsilon_{\text{error}} = 0$  corresponds to the perfect CSI case. It is observed that the beampattern gain obtained by different  $N$  and  $\epsilon_{\text{error}}$  monotonically increases with  $M$ . This observation shows that by carefully designing the BS beamformers and the IRS phase shifts, the system performance can still be improved with imperfect CSI even with large channel estimation errors, e.g.,  $\epsilon_{\text{error}} = 0.05$ . Furthermore, we observe that for a fixed  $M$ , the beampattern gain increases with  $N$ . This is due to the fact that more DoFs can be exploited for resource allocation to achieve higher array gain.

## VI. CONCLUSION

In this paper, we proposed the use of IRS to achieve simultaneous secure communication and sensing in the presence of an eavesdropping target and multiple communication users. The communication beamformers, the radar beamformers, and the IRS phase shifts were jointly optimized to maximize the sensing beampattern gain while satisfying the minimum SINR required by the users and secrecy constraint for the eavesdropping target. For the first scenario where the CSI of the user links

and the target location are known, a penalty-based algorithm was proposed to solve the formulated non-convex optimization problem. In particular, the beamformers were obtained via a semi-closed-form solution using the Lagrange duality method and the IRS phase shifts were obtained in closed-form by applying the MM method. For the second scenario where the CSI and the target location are imprecisely unknown, an efficient AO algorithm based on the  $\mathcal{S}$ -procedure and sign-definiteness approaches was proposed. Simulation results verified the effectiveness of the proposed scheme in achieving a flexible trade-off between the communication quality and the target sensing quality and showed the capability of the IRS for use in sensing and improving the physical layer security of ISAC systems. In addition, simulation results also illustrated the benefits of using dedicated sensing signals to improve the sensing quality.

## REFERENCES

- [1] A. Liu *et al.*, "A survey on fundamental limits of integrated sensing and communication," *IEEE Commun. Surveys Tuts.*, 2022, early access, doi: 10.1109/COMST.2022.3149272.
- [2] L. Zheng, M. Lops, Y. C. Eldar, and X. Wang, "Radar and communication coexistence: An overview: A review of recent methods," *IEEE Signal Process. Mag.*, vol. 36, no. 5, pp. 85–99, Sept. 2019.
- [3] F. Liu *et al.*, "Integrated sensing and communications: Towards dual-functional wireless networks for 6G and beyond," *IEEE J. Sel. Areas Commun.*, 2022, early access, doi: 10.1109/JSAAC.2022.3156632.
- [4] J. A. Zhang *et al.*, "Enabling joint communication and radar sensing in mobile networks—A survey," *IEEE Commun. Surveys Tuts.*, vol. 24, no. 1, pp. 306–345, 4th Quart. 2022.
- [5] C. Sturm and W. Wiesbeck, "Waveform design and signal processing aspects for fusion of wireless communications and radar sensing," *Proc. IEEE*, vol. 99, no. 7, pp. 1236–1259, Jul. 2011.
- [6] A. Hassanien *et al.*, "Dual-function radar-communications: Information embedding using sidelobe control and waveform diversity," *IEEE Trans. Signal Process.*, vol. 64, no. 8, pp. 2168–2181, Apr. 2016.
- [7] X. Liu, T. Huang, N. Shlezinger, Y. Liu, J. Zhou, and Y. C. Eldar, "Joint transmit beamforming for multiuser MIMO communications and MIMO radar," *IEEE Trans. Signal Process.*, vol. 68, pp. 3929–3944, Jun. 2020.
- [8] F. Liu, L. Zhou, C. Masouros, A. Li, W. Luo, and A. Petropulu, "Toward dual-functional radar-communication systems: Optimal waveform design," *IEEE Trans. Signal Process.*, vol. 66, no. 16, pp. 4264–4279, Aug. 2018.
- [9] H. Hua, J. Xu, and T. X. Han, "Optimal transmit beamforming for integrated sensing and communication," 2021. [Online]. Available: <https://arxiv.org/abs/2104.11871>.
- [10] K. Meng *et al.*, "Throughput maximization for UAV-enabled integrated periodic sensing and communication," 2021. [Online]. Available: <https://arxiv.org/abs/2203.06358>.
- [11] Z. Lyu, G. Zhu, and J. Xu, "Joint maneuver and beamforming design for UAV-enabled integrated sensing and communication," 2021. [Online]. Available: <https://arxiv.org/abs/2110.02857>.
- [12] K. Meng *et al.*, "UAV trajectory and beamforming optimization for integrated periodic sensing and communication," *IEEE Wireless Commun. Lett.*, 2022, early access, doi: 10.1109/LWC.2022.3161338.
- [13] Q. Wu *et al.*, "A comprehensive overview on 5G-and-beyond networks with UAVs: From communications to sensing and intelligence," *IEEE J. Sel. Areas Commun.*, vol. 39, no. 10, pp. 2912–2945, Oct. 2021.
- [14] Q. Wu and R. Zhang, "Towards smart and reconfigurable environment: Intelligent reflecting surface aided wireless network," *IEEE Commun. Mag.*, vol. 58, no. 1, pp. 106–112, Jan. 2020.
- [15] C. Pan *et al.*, "An overview of signal processing techniques for RIS/IRS-aided wireless systems." [Online]. Available: <https://arxiv.org/abs/2112.05989>.
- [16] Q. Wu and R. Zhang, "Beamforming optimization for wireless network aided by intelligent reflecting surface with discrete phase shifts," *IEEE Trans. Commun.*, vol. 68, no. 3, pp. 1838–1851, Mar. 2020.
- [17] G. Chen, Q. Wu, W. Chen, D. W. K. Ng, and L. Hanzo, "IRS-aided wireless powered MEC systems: TDMA or NOMA for computation offloading?" 2021. [Online]. Available: <https://arxiv.org/abs/2108.06120>.
- [18] T. Bai *et al.*, "Latency minimization for intelligent reflecting surface aided mobile edge computing," *IEEE J. Sel. Areas Commun.*, vol. 38, no. 11, pp. 2666–2682, Nov. 2020.
- [19] G. Chen, Q. Wu, C. He, W. Chen, J. Tang, and S. Jin, "Active IRS aided multiple access for energy-constrained IoT systems," 2022. [Online]. Available: <https://arxiv.org/abs/2201.12565>.
- [20] Q. Wu and R. Zhang, "Joint active and passive beamforming optimization for intelligent reflecting surface assisted SWIPT under QoS constraints," *IEEE J. Sel. Areas Commun.*, vol. 38, no. 8, pp. 1735–1748, Aug. 2020.
- [21] Z. Chu *et al.*, "A novel transmission policy for intelligent reflecting surface assisted wireless powered sensor networks," *IEEE J. Sel. Areas Commun.*, vol. 15, no. 5, pp. 1143–1158, Aug. 2021.
- [22] Q. Wu, X. Zhou, and R. Schober, "IRS-assisted wireless powered NOMA: Do we really need different phase shifts in DL and UL?" *IEEE Wireless Commun. Lett.*, vol. 10, no. 7, pp. 1493–1497, Jul. 2021.
- [23] M. Hua and Q. Wu, "Joint dynamic passive beamforming and resource allocation for IRS-aided full-duplex WPCN," *IEEE Trans. Wireless Commun.*, vol. 21, no. 7, pp. 4829–4843, Jul. 2022.
- [24] C. Pan *et al.*, "Multicell MIMO communications relying on intelligent reflecting surfaces," *IEEE Trans. Wireless Commun.*, vol. 19, no. 8, pp. 5218–5233, Aug. 2020.
- [25] H. Xie, J. Xu, and Y.-F. Liu, "Max-min fairness in IRS-aided multicell MISO systems with joint transmit and reflective beamforming," *IEEE Trans. Wireless Commun.*, vol. 20, no. 2, pp. 1379–1393, Feb. 2021.
- [26] M. Hua, Q. Wu, D. W. K. Ng, J. Zhao, and L. Yang, "Intelligent reflecting surface-aided joint processing coordinated multipoint transmission," *IEEE Trans. Commun.*, vol. 69, no. 3, pp. 1650–1665, Mar. 2021.
- [27] S. Buzzi, E. Grossi, M. Lops, and L. Venturino, "Foundations of MIMO radar detection aided by reconfigurable intelligent surfaces," *IEEE Trans. Signal Process.*, vol. 70, pp. 1749–1763, Mar. 2022.
- [28] W. Lu *et al.*, "Target detection in intelligent reflecting surface aided distributed MIMO radar systems," *IEEE Sensors Lett.*, vol. 5, no. 3, pp. 1–4, Mar. 2021.
- [29] X. Shao, C. You, W. Ma, X. Chen, and R. Zhang, "Target sensing with intelligent reflecting surface: Architecture and performance," 2022. [Online]. Available: <https://arxiv.org/abs/2201.09091>.
- [30] Z.-M. Jiang *et al.*, "Intelligent reflecting surface aided dual-function radar and communication system," *IEEE Systems J.*, 2021, early access, doi: 10.1109/JSYST.2021.3057400.
- [31] X. Song *et al.*, "Joint transmit and reflective beamforming for IRS-assisted integrated sensing and communication," 2021. [Online]. Available: <https://arxiv.org/abs/2111.13511>.
- [32] X. Wang *et al.*, "Joint waveform design and passive beamforming for RIS-aided dual-functional radar-communication system," *IEEE Trans. Veh. Technol.*, vol. 70, no. 5, pp. 5131–5136, May 2021.
- [33] R. Liu, M. Li, Y. Liu, Q. Wu, and Q. Liu, "Joint transmit waveform and passive beamforming design for RIS-aided DFRC systems," 2021. [Online]. Available: <https://arxiv.org/abs/2112.08861>.
- [34] R. Sankar and S. P. Chepuri, "Beamforming in hybrid RIS assisted integrated sensing and communication systems," 2022. [Online]. Available: <https://arxiv.org/abs/2203.05902>.
- [35] N. Su *et al.*, "Secure radar-communication systems with malicious targets: Integrating radar, communications and jamming functionalities," *IEEE Trans. Wireless Commun.*, vol. 20, no. 1, pp. 83–95, Jan. 2020.
- [36] —, "Secure dual-functional radar-communication transmission: Exploiting interference for resilience against target eavesdropping," *IEEE Trans. Wireless Commun.*, 2022, early access, doi: 10.1109/TWC.2022.3156893.
- [37] C. Hu, L. Dai, S. Han, and X. Wang, "Two-timescale channel estimation for reconfigurable intelligent surface aided wireless communications," *IEEE Trans. Commun.*, vol. 69, no. 11, pp. 7736–7747, Nov. 2021.
- [38] X. Yu, D. Xu, Y. Sun, D. W. K. Ng, and R. Schober, "Robust and secure wireless communications via intelligent reflecting surfaces," *IEEE J. Sel. Areas Commun.*, vol. 38, no. 11, pp. 2637–2652, Nov. 2020.
- [39] G. Zhou *et al.*, "A framework of robust transmission design for IRS-aided MISO communications with imperfect cascaded channels," *IEEE Trans. Signal Process.*, vol. 68, pp. 5092–5106, Aug. 2020.
- [40] S. Boyd and L. Vandenberghe, *Convex Optimization*. Cambridge University Press, 2004.
- [41] Y. Sun, P. Babu, and D. P. Palomar, "Majorization-minimization algorithms in signal processing, communications, and machine learning," *IEEE Trans. Signal Process.*, vol. 65, no. 3, pp. 794–816, Feb. 2017.
- [42] S. Boyd, L. El Ghaoui, E. Feron, and V. Balakrishnan, *Linear matrix inequalities in system and control theory*. Philadelphia, PA, USA: SIAM, 1994.
- [43] E. A. Gharavol and E. G. Larsson, "The sign-definiteness lemma and its applications to robust transceiver optimization for multiuser MIMO systems," *IEEE Trans. Signal Process.*, vol. 61, no. 2, pp. 238–252, Jan. 2013.
- [44] M. Shao, Q. Li, W.-K. Ma, and A. M.-C. So, "A framework for one-bit and constant-envelope precoding over multiuser massive MISO channels," *IEEE Trans. Signal Process.*, vol. 67, no. 20, pp. 5309–5324, Oct. 2019.